CENTRO DE INVESTIGACIÓN EN MATERIALES AVANZADOS S.C.

DEPARTAMENTO DE ESTUDIOS DE POSGRADO

Graduate School

Synthesis and structural and mechanical analysis of geopolymeric materials

(Síntesis y análisis estructural y mecánico de materiales geopoliméricos)

THESIS SUBMITTED IN PARTIAL FULLMILMENT OF THE REQUIREMENTS FOR THE DEGREE OF MASTER IN MATERIALS SCIENCE

PRESENTED BY:

Eng. Olga Idalu Perez Ordoñez

ADVISOR:

Jose Martin Herrera Ramirez, Ph.D.

CO-ADVISOR:

Luis Edmundo Fuentes Cobas, Ph.D.

CHIHUAHUA, CHIH. **August, 2017**

AKNOWLEDGMENTS

Undertaking this master has been truly life-changing experience for me and it would not have been possible to do without the support and guidance that I received from many people.

First of all I would like to thank God for everything he gave me.

I would like to express my gratitude to my advisor, Dr. J. Martin Herrera, and co-advisor, Dr. Luis E. Fuentes whose expertise, understanding and patience, considerably contributed to my graduate experience. I appreciate their vast knowledge and skill in many areas, and their assistance in writing reports (i.e., congress abstracts, scholarship applications and this thesis).

Special thanks to Dr. Francisco C. Robles at University of Houston for taking me into his group and for all the help, motivation and guidance during my research stay.

I would also like to thank my family for the support they provided me through my entire life and, in particular, I must acknowledge my parents for their support, patience and motivation.

Thanks to my mates at CIMAV: Armando Tejeda, Omar Velazquez, Graciela Alonso, Delfin Franco, Efrain Chacon, Claudia Chavez, Marco Merino and Ernesto Ledezma, for their valuable help and insightful comments.

I would also like to thank all my teachers at CIMAV for all the lessons taught and help whenever I needed it and to all the technicians at CIMAV who helped me during this project.

Special thanks to GCC for its support in lending equipment which was very helpful for the development of this research. In the same manner, I would like to thank to Dr. Carolina Prieto for her guidance and recommendations during the course of this work. Thanks also to Eng. Ceiry P. Alvidrez, Eng. David Soto and Eng. Tomas Martinez for their assistance in the manipulation of equipment.

In conclusion, I recognize that this research would not have been possible without the financial support of CONACYT and CIMAV during this project, as well as for performing a research stay at the College of Technology at the University of Houston; I express my gratitude to them.

CONTENTS

LIST OF FIGURES v

LIST OF TABLES vi

ABSTRACT 1

RESUMEN 2

JUSTIFICATION 3

Environmental problematic in the construction industry. 3

Mechanical and structural properties of geopolymers. 3

CHAPTER I: BACKGROUND 5

1.1 Portland cement. 5

1.2 Geopolymeric cement 7

1.2.1 History of geopolymer technology 7

1.2.2 Geopolymer impact. 7

1.2.3 Aluminosilicate polymerization. 8

1.2.4 Geopolymer applications. 9

1.2.5 Geopolymers as building materials. 10

1.2.6 Cost comparison between geopolymers and Portland cement. 11

1.3 Rietveld method. 11

HYPOTHESIS AND OBJECTIVES 13

Hypothesis. 13

Objectives 13

General objective 13

Specific objectives 13

CHAPTER 2: EXPERIMENTAL METHODOLOGY 14

2.1 Raw materials. 14

2.2 Characterization techniques. 15

2.2.1 Particle size distribution. 15

2.2.2 Scanning electron microscopy (SEM). 15

2.2.3 Thermal analysis by TGA-DSC. 15

2.2.4 Fourier transform infrared spectroscopy (FTIR). 16

2.2.5 Surface area and porosity (B.E.T.) 16

2.2.6 X-ray fluorescence (XRF). 16

2.2.7 X-ray diffraction (XRD). 16

2.2.8 Compressive strength. 17

2.3 Synthesis of geopolymeric and ordinary materials. 18

2.3.1 Synthesis of geopolymeric materials. 18

2.3.2 Synthesis of ordinary materials. 20

CHAPTER 3: RESULTS AND DISCUSSION 21

3.1 Characterization of the raw materials. 21

3.1.1 Particle size distribution. 21

3.1.2 Scanning electron microscopy. 22

3.1.3 Thermal analyses (TGA-DSC). 26

3.1.4 Fourier transform infrared spectroscopy. 30

3.1.5 Surface area and porosity (B.E.T.). 34

3.1.6 X-ray fluorescence. 35

3.1.7 X-ray diffraction. 37

3.1.8 Rietveld analyses. 42

3.2 Geopolymeric and ordinary pastes. 47

3.2.1 Compressive strength. 47

3.2.1.1 Effect of the particle size of clinker on the compressive strength. ... 50

3.2.1.2 Effect of dissolving the Pentasil® and/or sodium silicate in water on the compressive strength. ... 52

3.2.2 X-ray diffraction. ... 55

3.2.3 Rietveld analyses. ... 58

3.3 Geopolymeric and ordinary mortars. ... 60

3.3.1 Compressive strength. ... 60

3.3.1.1 Effect of the particle size of clinker on the compressive strength. ... 64

3.3.1.2 Effect of dissolving the Pentasil® and/or sodium silicate in water on the compressive strength. ... 66

3.3.2 X-ray diffraction. ... 70

CONCLUSIONS AND FUTURE WORK ... 74

Conclusions. ... 74

Future work. ... 75

REFERENCES ... 76

LIST OF FIGURES

Figure 1. *Compressive strength of a geopolymeric and an ordinary paste at different temperatures [4].* *4*

Figure 2. *Flow sketching of the production of (a) ordinary Portland cement and (b) a geopolymer.* *6*

Figure 3. *Particle size of the raw materials.* *21*

Figure 4. *SEM micrographs of the raw materials (continued on next page).* *23*

Figure 5. *Thermal analyses of the raw materials by TGA/DSC (continued on next page).* *27*

Figure 6. *FTIR results of the raw materials (continued on next page).* *31*

Figure 7. *Surface area of the raw materials.* *35*

Figure 8. *XRD patterns of the raw materials (continued on next page).* *37*

Figure 9. *Rietveld refinement of the raw materials (continued on next page).* *44*

Figure 10. *Semi-crystalline patterns.* *46*

Figure 11. *Compressive strength of the geopolymeric and ordinary pastes (continued on next page).* *48*

Figure 12. *Compressive strength by reducing clinker particle size to 15 and 130 µm of the pastes (continued on next page).* *51*

Figure 13*. Compressive strength with Pentasil® and/or sodium silicate dissolved and undissolved in water of the pastes (continued on next page).* *53*

Figure 14. *XRD patterns of the geopolymeric pastes (continued on next page).* *56*

Figure 15. *Rietveld refinement of the geopolymeric pastes (continued on next page).* *59*

Figure 16. *Compressive strength of the geopolymeric and ordinary mortars (continued on next page).* *61*

Figure 17. *Compressive strength by reducing clinker particle size to 15 and 130 µm of the mortars (continued on next page).* *65*

Figure 18. *Compressive strength with Pentasil® and/or sodium silicate dissolved and undissolved in water of the mortars (continued on next page).* *67*

Figure 19. *XRD patterns of the geopolymeric mortars (continued on next page).* *71*

LIST OF TABLES

Table 1. *XRD analyzes conditions.* *16*

Table 2. *Composition of geopolymeric materials in wt%.* *19*

Table 3. *Mixing program.* *19*

Table 4. *Composition of ordinary materials in wt%.* *20*

Table 5. *EDS analyzes of the aluminosilicates and Portland cement.* *25*

Table 6. *EDS analyzes of the activators and the sand.* *25*

Table 7. *Composition in oxides of the raw materials in wt% determined by XRF.* *36*

Table 8. *XRD patterns information of the raw materials.* *41*

Table 9. *Rietveld analyses results of the raw materials.* *43*

Table 10. *XRD pattern information of the geopolymeric pastes.* *55*

Table 11. *Rietveld analyzes results of the geopolymeric pastes.* *58*

Table 12. *XRD pattern information of the geopolymeric mortars.* *70*

ABSTRACT

Geopolymers could be a promising application of the cement industry as an alternative binder of the Portland cement, which is responsible of 8-10 wt% of the anthropogenic emissions of CO_2. Geopolymers could help to reduce the emissions that contribute to the greenhouse effect and improve mechanical and structural properties that actually an ordinary Portland cement has. In this research work, it was studied the raw materials by structural and microstructural analysis including, but not limited to, thermal analysis, scanning electron microscopy, particle size distribution, X-ray diffraction, X-ray fluorescence, surface area by the method BET and Fourier transform infrared spectroscopy. Subsequently the geopolymeric and ordinary materials were synthesized through ten different formulations; these materials were prepared in the form of pastes and mortars according to the ASTM C109/C109M-11 standard, which indicates that the material must be set in a 5 cm-side cubic mold. Once the materials were set, they were cured in a humid environment to complete the reaction that is carried out during curing; this procedure was performed according to the aforementioned standard. After 7, 14 and 28 days of curing, the pastes and mortars were tested by compression tests based on the ASTM E9 standard. The geopolymers were structurally studied by X-ray diffraction, and the geopolymeric pastes were analyzed by the Rietveld method. The results of this investigation showed that the compressive strength of the geopolymers increases with increasing the amount of the alite phase because it acts as a nucleating agent to promote the geopolymerization reaction. The geopolymers matched the compressive strength of ordinary material, which is extremely favorable since it has been shown that the production of the geopolymer generates a lower amount of greenhouse gases.

RESUMEN

Los geopolímeros parecen ser una aplicación prometedora en la industria del cemento como un aglomerante alternativo al cemento Portland, el cual es responsable del 8-10% de las emisiones antropogénicas de CO_2. Los geopolímeros podrían ayudar a reducir las emisiones que contribuyen al efecto invernadero y mejorar las propiedades mecánicas y estructurales que actualmente tiene un cemento Portland ordinario. En este trabajo de investigación se estudió la materia prima mediante análisis estructural y microestructural incluyendo, pero no limitados a, análisis térmicos, microscopía electrónica de barrido, distribución de tamaño de partícula, difracción de rayos X, fluorescencia de rayos X, área superficial por el método BET y espectroscopía de infrarrojo por transformada de Fourier. Posteriormente se sintetizaron los materiales geopoliméricos y ordinarios mediante diez formulaciones distintas; estos materiales fueron preparados en forma de pastas y morteros de acuerdo a la norma ASTM C109/C109M-11, la cual indica que el material debe de fraguar en un molde cúbico de 5 cm de lado. Una vez fraguados los materiales, se dejaron curar en un ambiente húmedo para completar la reacción que se lleva a cabo durante el curado; este procedimiento se realizó de acuerdo con la norma mencionada anteriormente. Después de 7, 14 y 28 días de curado, las pastas y morteros fueron ensayados mediante pruebas de compresión basados en la norma ASTM E9. Los geopolímeros fueron estudiados estructuralmente mediante difracción de rayos X, y las pastas geopoliméricas fueron analizadas mediante el método Rietveld. Los resultados de esta investigación mostraron que la resistencia a la compresión de los geopolímeros aumenta al incrementar la cantidad de la fase alita debido a que ésta actúa como un agente nucleante. Los geopolímeros igualaron la resistencia a la compresión de los materiales ordinarios, lo cual es sumamente favorable, ya que está demostrado que en la producción del geopolímero se genera una menor cantidad de gases de efecto invernadero.

JUSTIFICATION

Cement production is a major cause of climate change. Globally, its production has reached 2.8 billion tons per year and it is estimated to reach 4 billion tons per year in the coming years [1]. Therefore, it is looking to create new processes and ways to produce cement in order to be more sustainable as could be the case of the manufacture of geopolymers.

Environmental problematic in the construction industry.

In accordance with the International Energy Agency (IEA), Global CO_2 emissions will be approximately 28 billion tons in 2050. Emissions from cement production contribute with 8-10% of global emissions. Therefore, it is immediately required the reduction of this kind of pollution. Literature has reported that CO_2 emissions of the geopolymers, compared to the ordinary Portland cements (OPC), can be reduced by up to 80 wt% [2].

Mechanical and structural properties of geopolymers.

Kong and Sanjayan [3] compared the compressive strength between a geopolymeric paste, prepared by them, and an ordinary paste, which was made by Mendes and co-workers [4].

The results indicated that the geopolymeric paste reached a compressive strength of 58 MPa after heating it to a temperature of 800°C. On the other hand, the ordinary paste drastically reduced its compressive strength between temperatures of 400°C and 800°C, which was attributed to the presence of calcium hydroxide (Figure 1). Therefore, with these results, it can be proven that a geopolymer can have higher compressive strength than an OPC.

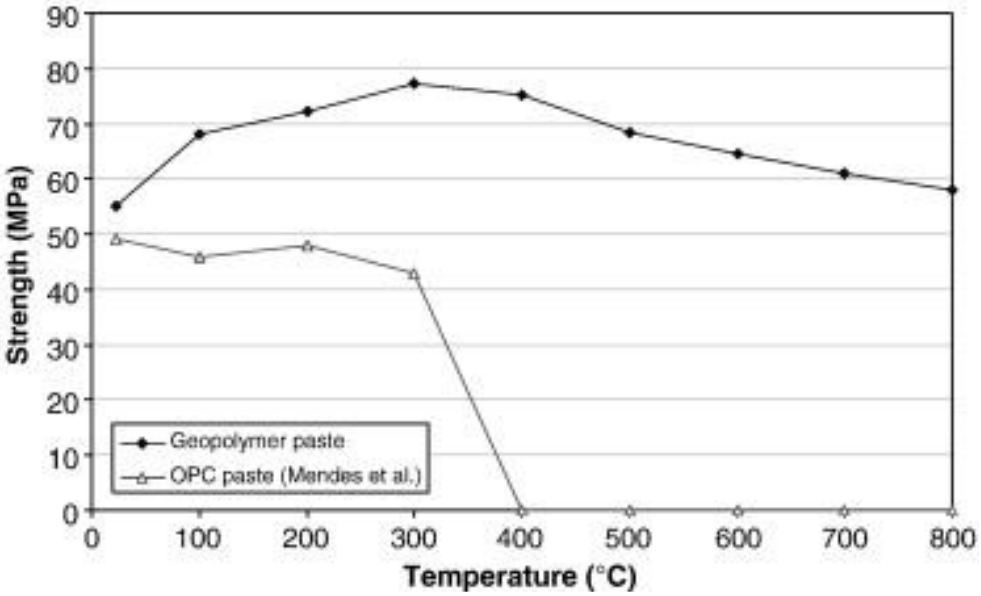

Figure 1. Compressive strength of a geopolymeric and an ordinary paste at different temperatures [4].

Structural analysis is important because it can explain the origin of properties from the crystalline structure level to the design of bulk materials. With a structural analysis, it is possible to present a unified treatment of the structure-property relationship from the level of a micrometric crystal (observing its interior to the detail of the unit cell), to the polycrystalline material [5].

Therefore, the structural analysis can determine the properties of the geopolymers in relation to its crystalline structure, such as mechanical properties, texture, chemical composition and crystalline phases.

CHAPTER I: BACKGROUND

This chapter is intended to perform a literature review based on what the Portland and geopolymer cements are, as well as their impact on the environment. Furthermore, a review of the Rietveld method is made in order to understand what the objective of this method is.

1.1 Portland cement.

Portland cement is known since long time ago and it is considered as the hydraulic binder most important in the world [6]. Its name comes from its greenish-gray color, similar to the rocks of the cliff of Portland, England [6, 7]. The volcanic ashes were discovered by the Greeks and Romans. They produced the first calcium silicate cement. If that cement is finely ground and mixed with lime and water, a hardened mortar is produced, which is resistant to weathering. The reaction that occurs in the mixture is called pozzolanic reaction and it is the responsible of giving the strength and performance to the concrete using materials such as fly ash, microsilica and metakaolin in modern concrete [8]. In essence, Portland cement is obtained from a kind of slag called "clinker", which is gotten by burning at around 1500°C a mixture of limestone and clay in definite proportions and finely pulverized. Then the clinker previously cooled and ground is mixed with small portions of gypsum that is used to control the curing speed to finally obtain Portland cement [6-8]. This procedure can be seen in Figure 2a.

The cement manufacturing process is expensive because a large amount of fuel to reach those temperatures is required. The main sources of the CO_2 emissions in the OPC are attributed to the calcination of limestone. The CO_2 generated is a by-product of calcinations and fuels burned during the cement manufacturing [9, 10].

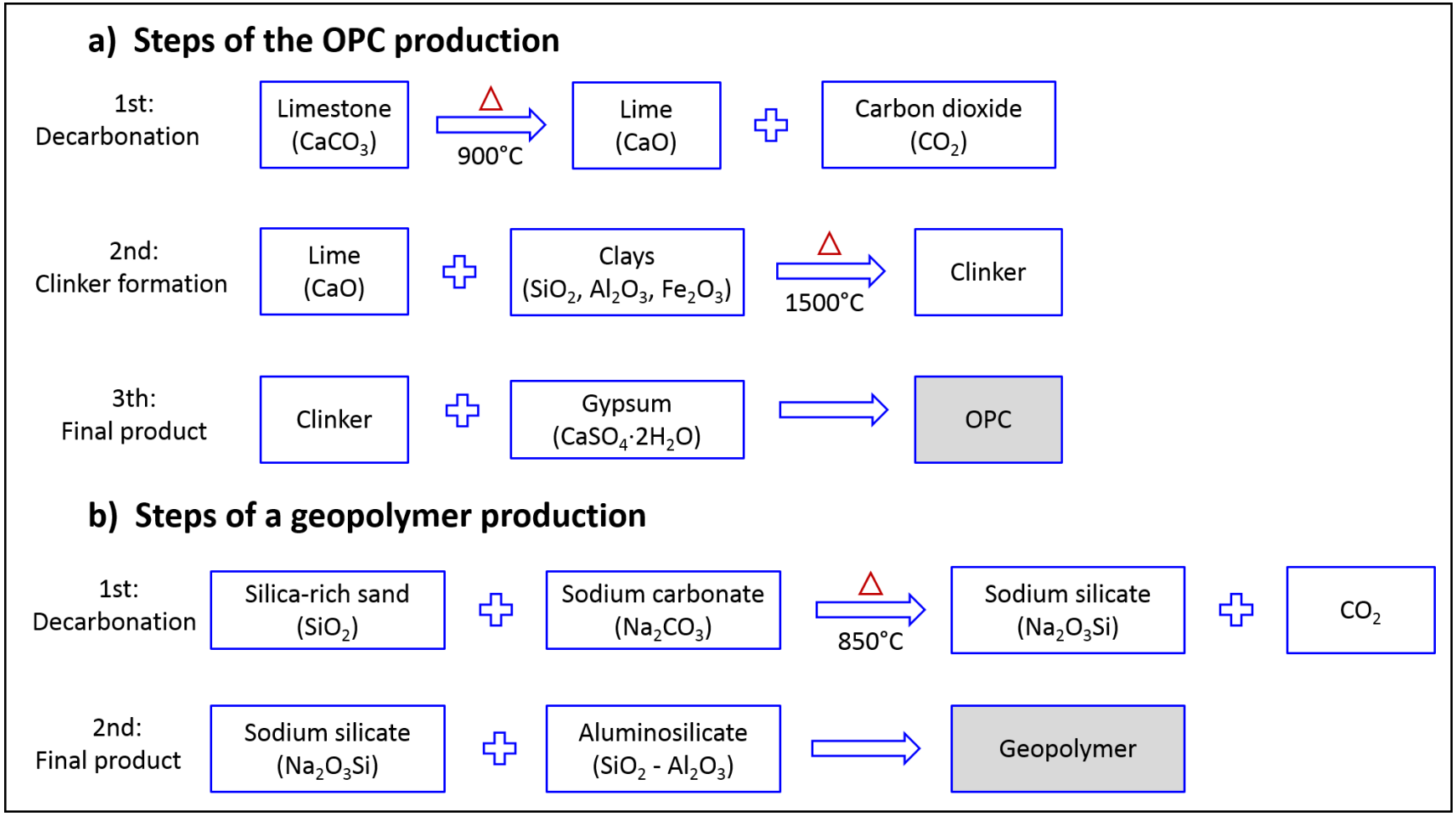

Figure 2. Flow sketching of the production of (a) ordinary Portland cement and (b) a geopolymer.

1.2 Geopolymeric cement

1.2.1 History of geopolymer technology

The term “geopolymer” (aluminosilicate polymer) was coined in the 1970s by the French scientist and engineer Prof. Joseph Davidovits [9]. Geopolymer is a type of solid material synthesized by the reaction of an aluminosilicate powder with an alkaline solution. The primary application for geopolymer binder is for construction. It is possible to generate reliable and high-performance geopolymers by alkaline activation of fly ash or a by-product of coal combustion. The synthesis of construction materials by alkaline activation of solid non-Portland cement precursors (usually high-calcium metallurgical slags) was first demonstrated by Purdon in 1940 [9].

1.2.2 Geopolymer impact.

The concrete industry faces challenges to meet the growing demand of Portland cement due to limited reserves of limestone, slow manufacturing growth and increasing carbon taxes. The demand of cement has been increasing due to increased infrastructural activities of the world. In recent years, geopolymers have attracted considerable attention among these binders because of their early compressive strength, low permeability, good chemical resistance and excellent fire resistance behavior [11]. In this respect, geopolymers are an alternative cementitious binder, comprising of an alkali-activated fly ash, and they have been considered as a substitute for ordinary Portland cement (OPC). The cement hardens at room temperature and provides compressive strengths of 20 MPa after 4 h and up to 70-100 MPa after 28 days [12]. In addition, studies that have been completed on geopolymer concretes indicate that there is a potential for 25-45% or 70% reduction in greenhouse gas emissions [9, 10].

1.2.3 Aluminosilicate polymerization.

The raw material used to produce geopolymers may be one that contains high amounts of silica and alumina and small amounts of calcite and ferric oxide [13]. A geopolymer requires an alkaline activator to induce its pozzolanic property and to accelerate the geopolymerization process. In several studies, it has found that sodium silicate is a great activator of geopolymeric cement [9, 13-15]. For this reason, this research has been focused in obtaining geopolymers using sodium silicate. It is worth saying that this sodium silicate was produced at CIMAV at laboratory level and subsequently at pilot level starting from silica-rich sands [16].

Although the geopolymerization mechanism is not well understood, the most proposed mechanism includes four parallel stages [17]:

a) Closure of solid aluminosilicate materials in alkaline sodium silicate solution,
b) Oligomerization of Si and/or Si-Al in aqueous phase,
c) Polymerization of the oligomeric species, and
d) Bonding of undissolved solid particles in the polymer.

It is obvious that polymerization in sodium silicate solutions comprises a fundamental process in geopolymerization technology [17].

Aluminosilicate polymers consist of an amorphous, three-dimensional structure resulting from the polymerization of aluminosilicate monomers in an alkaline solution. The alkaline solution most often utilized is a sodium silicate solution, although potassium silicate solutions and other alkaline solutions have also been used. The composition of the final inorganic polymer can be altered by changing the chemistry of the activating solution.

Rahier and co-workers [18] reported a study on inorganic polymer formation and properties, and proposed the following polymerization reaction:

$$wNa_2O * xSiO_2 * yH_2O + Al_2O_3 * 2SiO_2 \xrightarrow{<100℃} wNa_2O * Al_2O_3 * (2+x)SiO_2 * zH_2O$$

where the values of *w*, *x* and *y* depend on the composition of the alkaline solution and *z* is the degree of hydration [18]. While the precise reaction paths are still unknown, Davidovits [14] has proposed a reaction pathway involving the polycondensation of hypothetical monomers, the orthosilicate ions, as shown below.

$$Al_2O_3 \cdot 2SiO_2 + 2nH_2O \xrightarrow{NaOH} n(OH)_3 - Si - O - Al^{(-)} - (OH)_3$$

$$n(OH)_3 - Si - O - Al^{(-)} - (OH)_3 \xrightarrow{NaOH} Na^{(+)} - \left(\begin{array}{c} | \\ Si \\ | \\ O \end{array} - O - \begin{array}{c} | \\ Al^{(-)} - O - \\ | \\ O \end{array} \right)_n + 3nH_2O$$

1.2.4 Geopolymer applications.

The principal application of geopolymer technology is currently in the development of CO_2-reduced construction materials as an alternative to Portland-based (calcium silicate) cements [9, 12]. Figure 2b shows the flow sketching to produce geopolymers. The first step consists in the synthesis of sodium silicate that could be made by the reaction of silica-rich sand and sodium carbonate; then it is mixed with the source of aluminosilicate to obtain the geopolymer. Other ways to synthesize sodium silicate is by reacting silica-rich sands with sodium hydroxide or sodium bicarbonate, as studied by Tejeda [16]. Geopolymers can be

also used for coatings and adhesives, new binders for fiber composites and waste encapsulation. The properties and uses of geopolymers are being explored in many scientific and industrial disciplines as modern inorganic chemistry, physical chemistry, colloid chemistry, mineralogy, geology, and in all types of engineering process technologies. The wide variety of potential applications includes: fire resistant materials, decorative stone artifacts, thermal insulation, low-tech building materials, low energy ceramic tiles, refractory items, thermal shock refractories, bio-technologies (materials for medicinal applications), foundry industry, cements and concretes, composites for infrastructures repair and strengthening, high-tech composites for aircraft interior and automobile, high-tech resins systems, radioactive and toxic waste containment, arts and decoration, cultural heritage, archeology and history of sciences [9, 13].

1.2.5 Geopolymers as building materials.

Some of the applications of geopolymers as building materials could be: cement pathways, pavers, mine backfill, railway sleepers (ties), sewerage pipes and earth retaining walls [19]. Geopolymers are produced from a source of aluminosilicates such as metakaolin, fly ash, ground granulated blast furnace slags and mineral processing wastes, requiring further a highly concentrated caustic silicate solution as an activator for geopolymers [19]. Sodium silicate is well known for its advantage as a geopolymer activator [9]. Therefore, it is not necessary to produce the source of aluminosilicates since it can be gotten from industry waste and the activator can be produced at a lower temperature than the required for producing OPC (Figure 2) [19]. One of the disadvantages of geopolymers is that they are usually cured at elevated temperatures (60-90°C) and it is impractical to thermally cure them for high volumes or in situ poured paths, roads and curbing [19]. Literature has reported that it is

possible to skip the thermal curing adding calcium-containing compounds such as lime or ground granulated blast furnace slag [19].

When the geopolymer is cured at high temperature, the strength increases since the geopolymerization degree is higher, and therefore the amount of reaction products increases.

On the other hand, when the geopolymer is developed at lower temperature, it grows slowly and therefore its quality is better in terms of lower porosity and higher toughness [20]. Van Deventer and co-workers suggested that the presence of calcium in solid waste materials will provide extra nucleation sites for precipitation of dissolved species and cause rapid hardening [21].

1.2.6 Cost comparison between geopolymers and Portland cement.

The production cost of geopolymers is very variable depending on the raw material used, source location, the energy source and the mode of transport [10]. The financial costs of geopolymers could be 7% lower than OPC [10]. Also, Duxon et. al. said that, for the case of geopolymer concrete derived from fly ash, the cost of the material is generally about 10–30% lower than OPC [22]. The OPC production cost also varies between US$ 35.00 and US$ 40.00 per ton of cement depending on the capacity [23]. Therefore, the production cost of one ton of geopolymer could vary between US$ 24.50 and US$ 37.20.

1.3 Rietveld method.

X-ray diffraction is a non-destructive testing method for determining a range of physical and chemical characteristics of materials. X-ray diffraction results from the interaction between X-rays and electrons of atoms. When the interaction of the incident monochromatic X-ray with the sample produces constructive interference, the Bragg's Law is satisfied:

$$n\lambda = 2d\ Sin\ \theta$$

where λ is the wavelength, n is the diffraction order, θ is the angle between the X-ray beam and the incidence plane and d is the interplanar distance [5].

The applications of X-ray diffraction include phase analysis, for example the type and quantities of phases present in the sample, the crystallographic unit cell and crystal structure, crystallographic texture, crystalline size, macro-stress and micro-strain, and also electron radial distribution functions [24].

Rietveld method was invented by the scientist Hugo Rietveld in the 1960s. Rietveld method is a refinement technique, it means, it is necessary an initial model to begin the work analysis [5]. The Rietveld method compares an experimental X-ray diffraction pattern with a calculated one based on the crystal structures of the various phases. The refinement procedure then minimizes the difference between them and calculates different measures of the fit [25].

The structure model is generally obtained from the monocrystalline method. The Rietveld polycrystalline method does not supplant the monocrystalline method, the former is a complement of the latter [5].

The disadvantage of the polycrystalline method is that the diffraction peaks overlap each other. This overlap occurs when the interplanar distances of different family of planes are roughly the same [5].

One of the advantages of the Rietveld method is the possibility of quantifying mineral phases in the presence of amorphous matter [26]. This capability was evaluated in this research work. A practical way to quantify the amorphous matter is considering a crystalline phase with a very small crystal size as the amorphous matter [27].

HYPOTHESIS AND OBJECTIVES

Hypothesis.

A structural analysis of geopolymers, with a significant component by the Rietveld method, will allow understanding their mechanical behavior under compressive loads.

Objectives

General objective

To produce and characterize a set of formulations of geopolymeric pastes and mortars in the region of compositions of interest.

To evaluation of the mechanical strength of the products obtained will be performed together with the identification of the main phases present in them, in order to establish the relationship between the structure and mechanical properties.

Specific objectives

- To characterize the raw material with which different geopolymeric and ordinary materials will be manufactured by different techniques.
- To synthesize geopolymeric materials with different compositions of metakaolin, natural silica with pozzolanic properties, clinker and sodium silicate.
- To synthesize ordinary materials with the same compositions as the geopolymeric materials using OPC.
- To characterize the geopolymers by compression tests and XRD.
- To characterize the ordinary materials by compression tests.
- To analyze the geopolymeric pastes by the Rietveld method.

CHAPTER 2: EXPERIMENTAL METHODOLOGY

The purpose of this chapter is to know the different raw materials, techniques, procedures and equipment used during this research work, as well as to detail how geopolymeric and ordinary materials will be synthesized.

2.1 Raw materials.

The raw materials used to make the geopolymeric and ordinary pastes and mortars were the following:

- **Metaforce®:** It is a metakaolin with high concentration of silica and aluminum oxide. It was used as a source of aluminosilicate for geopolymers.
- **Microsilex®:** It is a natural silica based product with pozzolanic properties used as a source of aluminosilicate for the production of geopolymers.
- **Clinker:** It is a kind of slag obtained from the calcination of limestone and clays at around 1500°C. It was used as the calcium-containing compound in order to avoid the thermal curing and as an aluminosilicate source for geopolymers.
- **Pentasil®:** It is sodium metasilicate pentahydrate that consists of a molecule of silicon oxide (SiO_2) and sodium oxide (Na_2O) and five water molecules. It was used as an activator for geopolymers.
- **Sodium silicate:** It is a compound used as an activator for geopolymers. It was obtained from the calcination of silica-rich sand and sodium carbonate in a pilot plant at around 850°C, as seen in Figure 2b.
- **Sodium hydroxide:** It is a compound with 98 wt% of purity brand Macron® used as an activator for geopolymers.
- **Ordinary Portland cement (OPC):** It is the mixture of clinker previously cooled and ground with small portions of gypsum; it was used to make the ordinary materials. This is a high quality OPC since the amount of calcium carbonate is too low, the commercial Portland cement contain between 30 and 40 wt%.
- **Ottawa® sand:** It is quartz that was used as a fine aggregate for making geopolymeric and ordinary mortars.

2.2 Characterization techniques.

2.2.1 Particle size distribution.

The particle size distribution of the raw materials was determined using a laser granulometer CILAS 1180. The samples were dissolved in isopropyl alcohol to have alcohol/aqueous suspensions (20:80).

This equipment uses the laser diffraction and a CCD camera, which allows, in one single range, the measurement of particles between 0.04 and 2,500 µm. The fine particles are measured by the diffraction pattern, using Fraunhofer or Mie theory. The coarse particles are measured using a real-time fast Fourier transform of the image obtained with a CCD camera equipped with a digital signal processing unit (DSP) [28].

2.2.2 Scanning electron microscopy (SEM).

A SEM Hitachi SU3500 was used to observe the morphology and particle size by a secondary electron detector, to distinguish the present phases by a backscattering electron detector and to do elementary analysis by energy-dispersive X-ray spectrometry (EDS) of the raw materials. The powders were placed on graphite tape. An ultra-fine coating of gold was applied on the sample surface to ensure the electron flow.

2.2.3 Thermal analysis by TGA-DSC.

A TA Instruments simultaneous thermal analyzer (TGA-DSC) was used to measure the heat flow and weight changes in the raw materials as a function of temperature under air atmosphere. The analysis was performed using a rate of 10°C/min until 900°C.

2.2.4 Fourier transform infrared spectroscopy (FTIR).

A Thermo/Nicolet Magna-IR 750 spectrometer was used for the purpose of knowing the functional groups present in the raw materials. A special sample preparation was no required.

2.2.5 Surface area and porosity (B.E.T.)

A Quantachrome Autosorb 1C surface area and pore size analyzer was used for knowing the area of contact that the raw materials will have to carry out the chemical reaction.

2.2.6 X-ray fluorescence (XRF).

Chemical oxide composition of the raw materials was determined by X-ray fluorescence. The equipment used for this analysis is an Epsilon 3^{XLE} energy dispersive X-ray fluorescence (EDXRF) spectrometer developed by PANalytical. Samples were compacted into a tablet of approximately 5 g to do the analysis.

2.2.7 X-ray diffraction (XRD).

An XRD analysis was made in order to know the present phases in each sample (raw materials and products) and to do the Rietveld method analysis. It was employed a PANalytical X'pert PRO diffractometer and the conditions to which analyzes were carried out are presented in Table 1. The software used to carry out the Rietveld method analyzes was FullProf Suite.

Table 1. XRD analyzes conditions.

Condition	Value
2θ range (degree)	10 to 80
Step (degree)	0.015
Time (s)	120
λ Cu K_α radiation (Å)	1.5418

2.2.8 Compressive strength.

The products were characterized by compression tests after 7, 14 and 28 days of curing. The tests were carried out in an INSTRON universal testing machine with a load cell of 50 tons. This technique was used with the purpose of knowing the mechanical properties of the material and to know the formulation with the higher, moderate and the lowest compressive strength.

2.3 Synthesis of geopolymeric and ordinary materials.

2.3.1 Synthesis of geopolymeric materials.

Table 2 shows the different formulations of geopolymers synthesized during this research work. As can be seen, the first four formulations are pastes, since they do not have sand, and the last 6 formulations are mortars. Formulation 4 was made according to the molar ratios of the paste with the highest compressive strength used by Barbosa and co-workers [29]. The procedure to make the geopolymers was:

1. The Metaforce®, Microsilex® and clinker were premixed until homogenization.
2. The Pentasil® or the sodium silicate were dissolved in distilled water used for each formulation. The sodium hydroxide was prepared in a 14 M solution for the formulation 4.
3. The mixture of the aluminosilicate sources (Metaforce®, Microsilex® and clinker) was placed into the mixer bowl.
4. The solutions of Pentasil®, sodium silicate and/or sodium hydroxide were slowly added to the mixture.
5. The mixer was operated at low speed and the sand was added during the first minute of mixing.
6. Subsequently, the mixing program indicated in Table 3 was followed.
7. The mixture was placed into cubic molds of 5 cm of side.
8. After 24 h of hardening, samples were placed inside of a 300 gauge plastic bag and then into a bucket with water to begin the curing process.

Table 2. Composition of geopolymeric materials in wt%.

Formulation	Sodium hydroxide	Microsilex®	Metaforce®	Pentasil®	Clinker	Sodium silicate	Sand	Water
F1	0.00	6.22	21.77	12.44	40.43	0.00	0.00	19.14
F2	0.00	6.22	21.77	0.00	40.43	12.44	0.00	19.14
F3	0.00	6.11	21.37	0.00	39.69	8.87	0.00	23.97
F4	23.20	0.00	57.64	16.48	0.00	0.00	0.00	2.68
F5	0.00	2.87	10.04	0.00	18.64	4.17	49.72	14.57
F6	0.00	2.97	10.38	2.97	19.28	2.96	52.31	9.13
F7	0.00	2.97	10.38	5.93	19.28	0.00	52.31	9.13
F8	0.00	2.97	10.38	0.00	19.28	4.31	51.42	11.65
F9	0.00	2.97	10.38	4.31	19.28	0.00	51.42	11.65
F10	0.00	2.97	10.38	0.00	19.28	5.93	52.31	9.13

Table 3. Mixing program.

Mixer speed	Time (s)	Comments
1	60	Addition of sand in case to be mortar
2	30	
Repose	60	
2	60	

2.3.2 Synthesis of ordinary materials.

Ordinary materials were made under the same conditions and using the same manufacturing process that was used for the geopolymer synthesis, in order to compare the mechanical properties of both kind of materials.

Table 2 and Table ***4*** show the composition of both, the geopolymeric materials and the ordinary materials, respectively. It should be considered that sodium hydroxide, Metaforce®, Microsilex®, Pentasil®, sodium silicate and/or clinker are the components of the geopolymer cement, therefore the amount of OPC used is the sum of the components mentioned.

Table 4. Composition of ordinary materials in wt%.

Formulation	OPC	Sand	Water
F1	80.86	0.00	19.14
F2	80.86	0.00	19.14
F3	76.04	0.00	23.97
F4	97.32	0.00	2.68
F5	35.72	49.72	14.57
F6	38.56	52.31	9.13
F7	38.56	52.31	9.13
F8	36.94	51.42	11.65
F9	36.94	51.42	11.65
F10	38.56	52.31	9.13

CHAPTER 3: RESULTS AND DISCUSSION

In this chapter the characterization results of the raw materials, as well as those of the synthesis of geopolymeric and ordinary materials will be presented and discussed.

3.1 Characterization of the raw materials.

3.1.1 Particle size distribution.

Figure 3 shows the average of raw material particle size. All the raw materials, except sand, must have similar particle size and as small as possible in order to be able to compare the mechanical properties of the synthesized materials. If the particle size is too big, the mechanical properties considerably fall due to the lack of compaction.

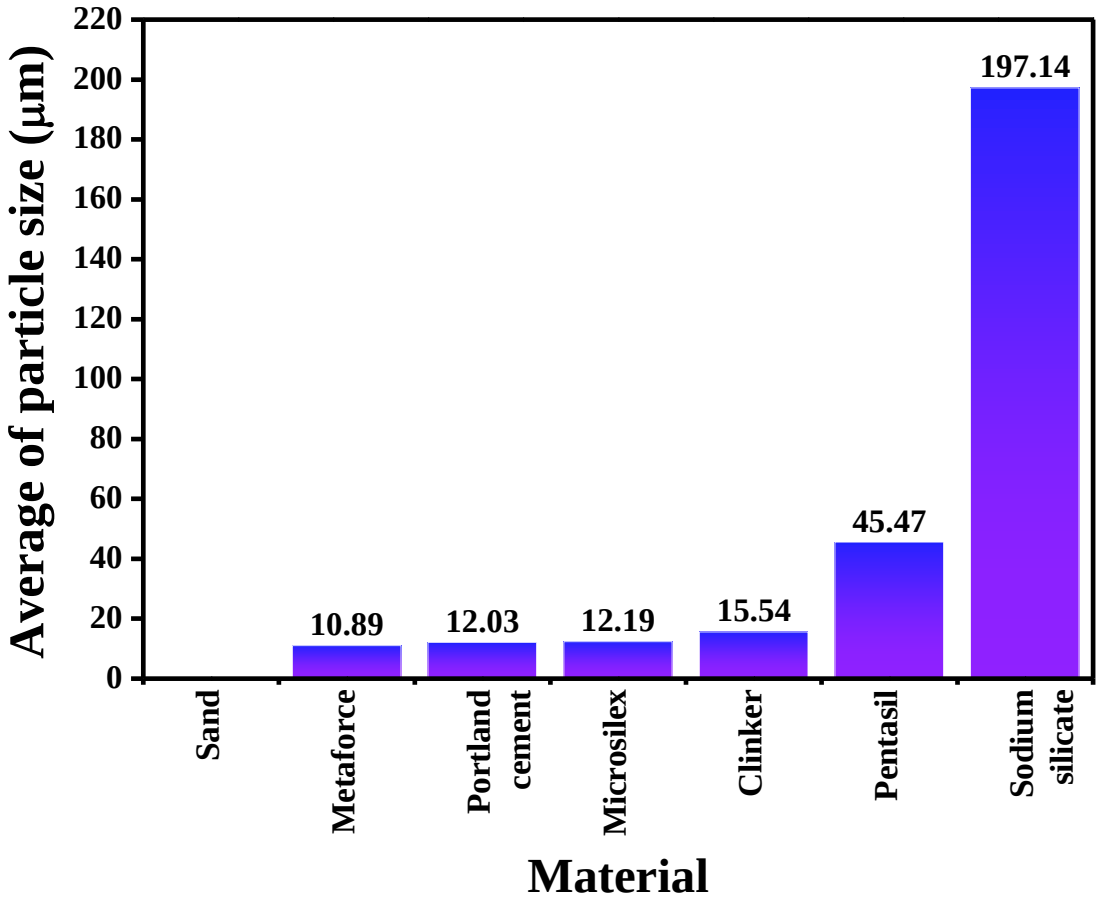

Figure 3. Particle size of the raw materials.

As can be observed in Figure 3, all the aluminosilicate sources and the Portland cement have a similar particle size, except the Pentasil® and sodium silicate. Pentasil® could not be ground because it left a chewy and doughy consistency. Sodium silicate agglomerated at the moment of the analysis. Because of this, it was decided to dissolve in water the Pentasil® and sodium silicate to synthesize the geopolymers. The large size of the sand did not affect the geopolymer synthesis, as it was used as fine aggregate in the case of mortars.

3.1.2 Scanning electron microscopy.

Figure 4 illustrates SEM micrographs of the raw materials. The micrographs from the left were acquired using a secondary electron signal to observe the morphology of the materials. The micrographs from the right were acquired using a backscattered electron signal to see the difference in contrast among compounds due to differences in atomic numbers. In general, the morphology of aluminosilicate sources and Portland cement displays a high size variation and irregular shapes. Pentasil® and sand show a big particle size distribution and porosity with the only difference that sand have a rounded shape and Pentasil® and irregular shape with sharpie corners. Finally, only the sodium silicate shows a fiber morphology and its tendency to agglomeration. Backscattered electron signal shows that there is no appreciable difference in contrast in the Pentasil®, sodium silicate and sand. In comparison, Portland cement, Metaforce®, Microsilex® and clinker have appreciable difference of contrast due to the presence of calcium.

Table 5 shows the EDS analyzes of the aluminosilicates and Portland cement. Portland cement and clinker have a similar composition since, as mentioned before, Portland cement is the mixture of clinker and gypsum. They represent a calcium-rich component, hence clinker was used as the calcium component in order to avoid applying a heat treatment during

the curing. Metaforce® was confirmed to be an aluminosilicate since its principal elements are silicon, aluminum and oxygen. Microsilex® could be proven to be a silica component because of the presence of oxygen and silicon.

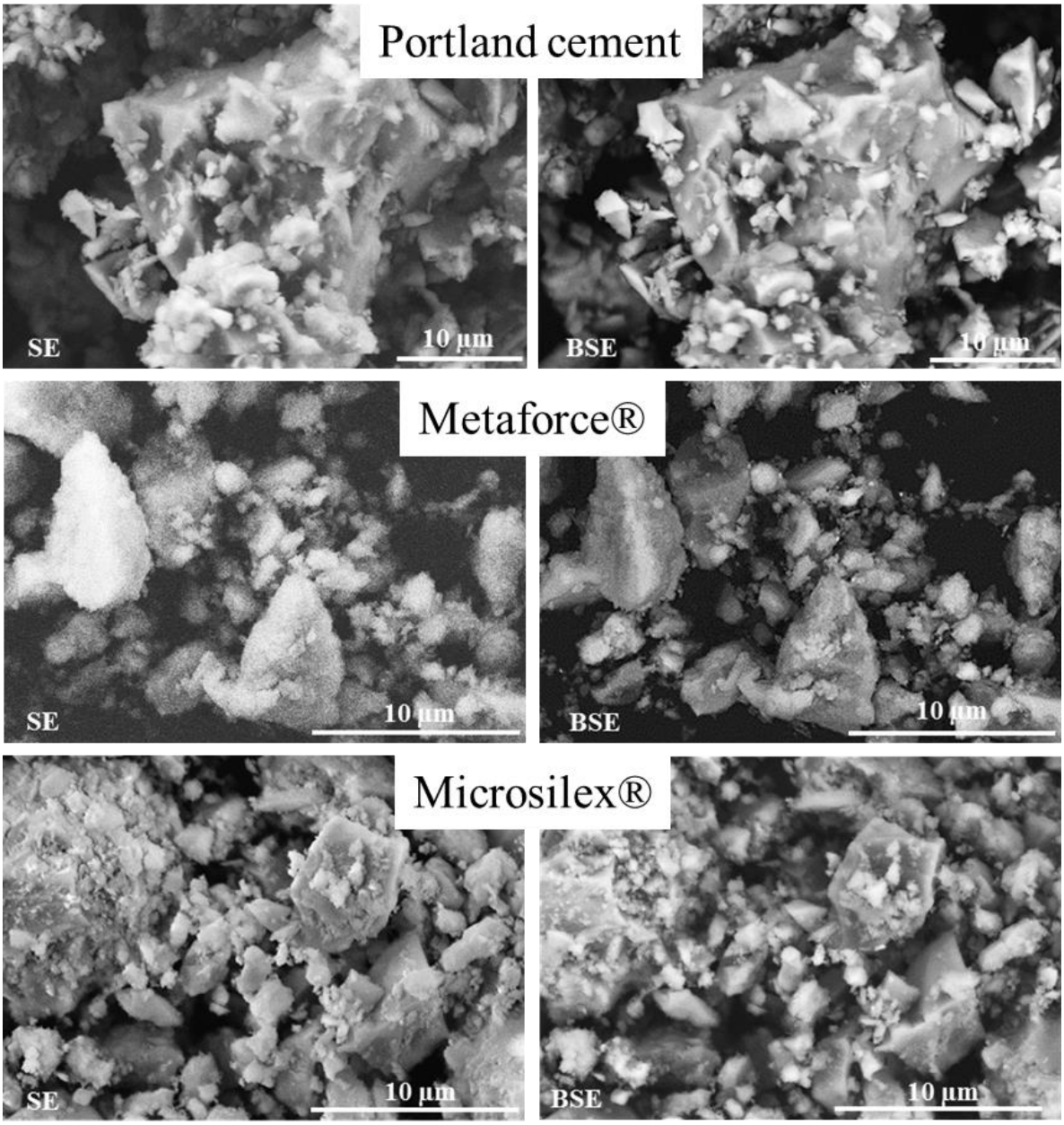

Figure 4. SEM micrographs of the raw materials (continued on next page).

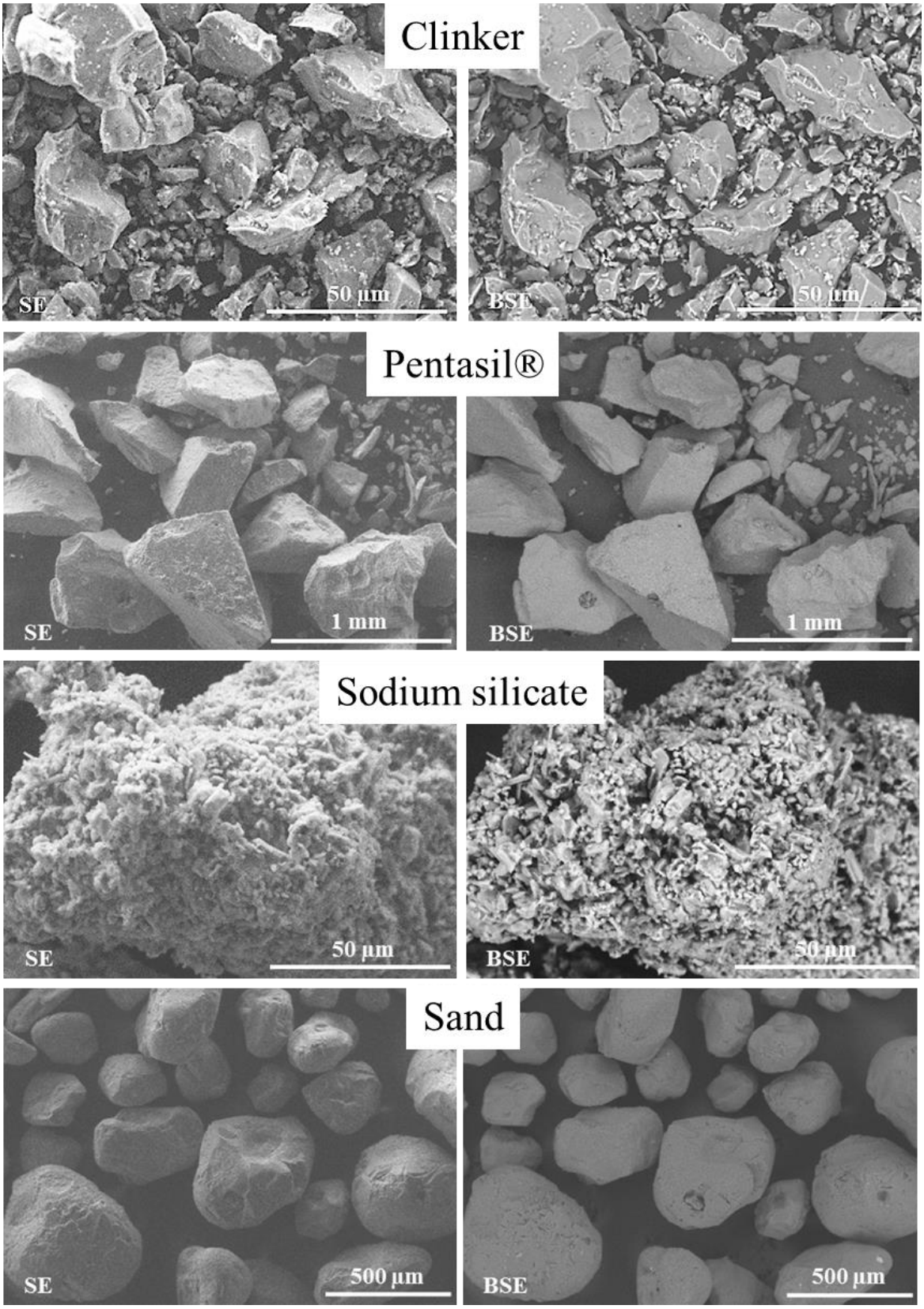

Figure 4 (continued). SEM micrographs of the raw materials.

Table 5. EDS analyzes of the aluminosilicates and Portland cement.

Element	Portland cement	Metaforce®	Microsilex®	Clinker
Ca	41.7	3.7	4.6	47.7
O	35.4	50.8	53.2	36.7
Al	9.5	16.6	2.2	3.2
Si	8.6	24.6	37.9	7.1

Table 6 displays the EDS analyses of the activators and the sand. As can be observed, activators are rich in sodium, oxygen and silicon since, as it is known, they are sodium silicates. The sand, as expected, has a large amount of silicon and oxygen because it is a silica-rich sand.

Table 6. EDS analyzes of the activators and the sand.

Element	Pentasil®	Sodium silicate	Sand
O	61.4	45.5	56.6
Na	24.0	37.3	43.0
Si	14.4	15.6	0.0

3.1.3 Thermal analyses (TGA-DSC).

In order to know the behavior of raw materials at high temperatures and to quantify the components present in each material, a simultaneous thermal analysis TGA/DSC was performed.

The results shown in Figure 5 revealed a first weight loss at around 100°C due to the presence of moisture. Pentasil® demonstrated to have a big weight loss (around 60 wt%) at this temperature because, as it was said before, it contents five molecules of water.

The second weight loss at around 450°C in clinker and Portland cement is due to the presence of less than 1 wt% of calcium hydroxide.

The last weight loss between 500 and 900°C corresponds to a decarbonation process. The temperature variation of this weight loss is due to the difference in particle size of the materials. In coarse particles, the decarbonation process is more difficult to succeed.

As can be seen, the amount of calcium carbonate in Portland cement is too low (less than 3 wt%). When the amount of calcium carbonate is low, the compressive strength will be high. Therefore, that quantity will determinate the quality of the Portland cement. In this case, as was said before, it is a high quality Portland cement.

The sand did not have any weight loss since, as its formula says (SiO_2), it only contains silica and cannot be degraded until very high temperatures (~ 4800°C). Silica, as it is known, is a ceramic material having the characteristic of being resistant to high temperatures [30].

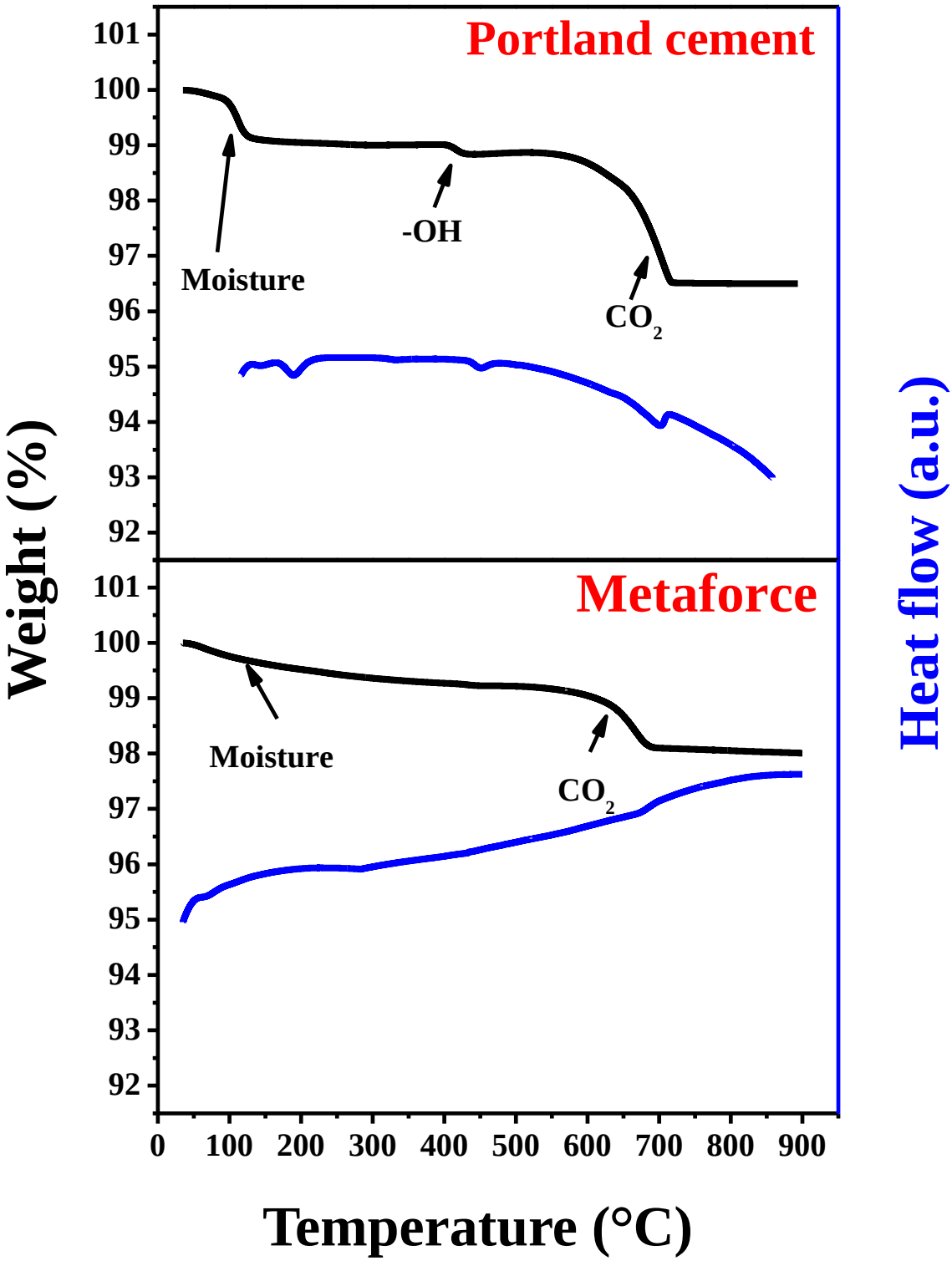

Figure 5. Thermal analyses of the raw materials by TGA/DSC (continued on next page).

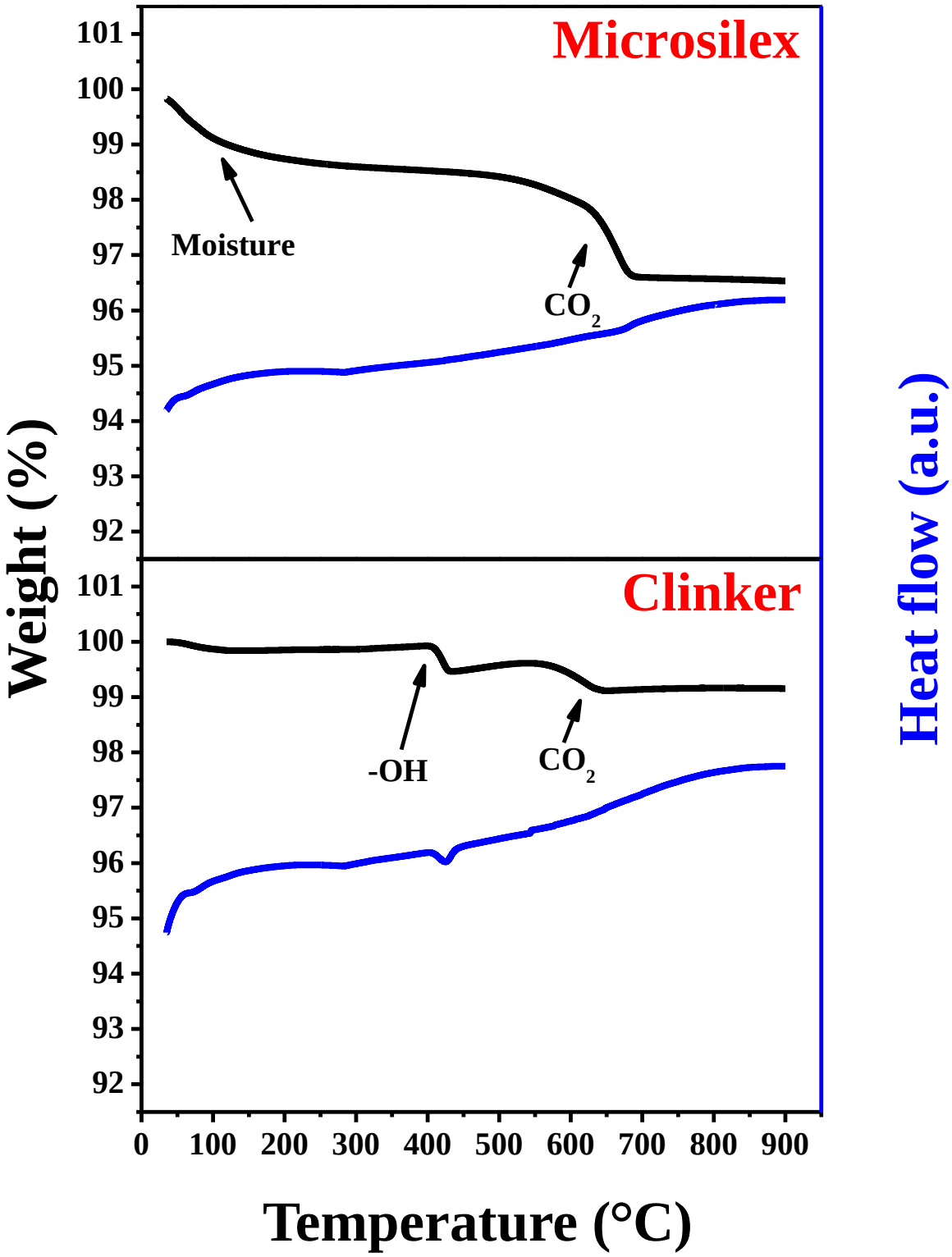

Figure 5 (continued). Thermal analyses of the raw materials by TGA/DSC (continued on next page).

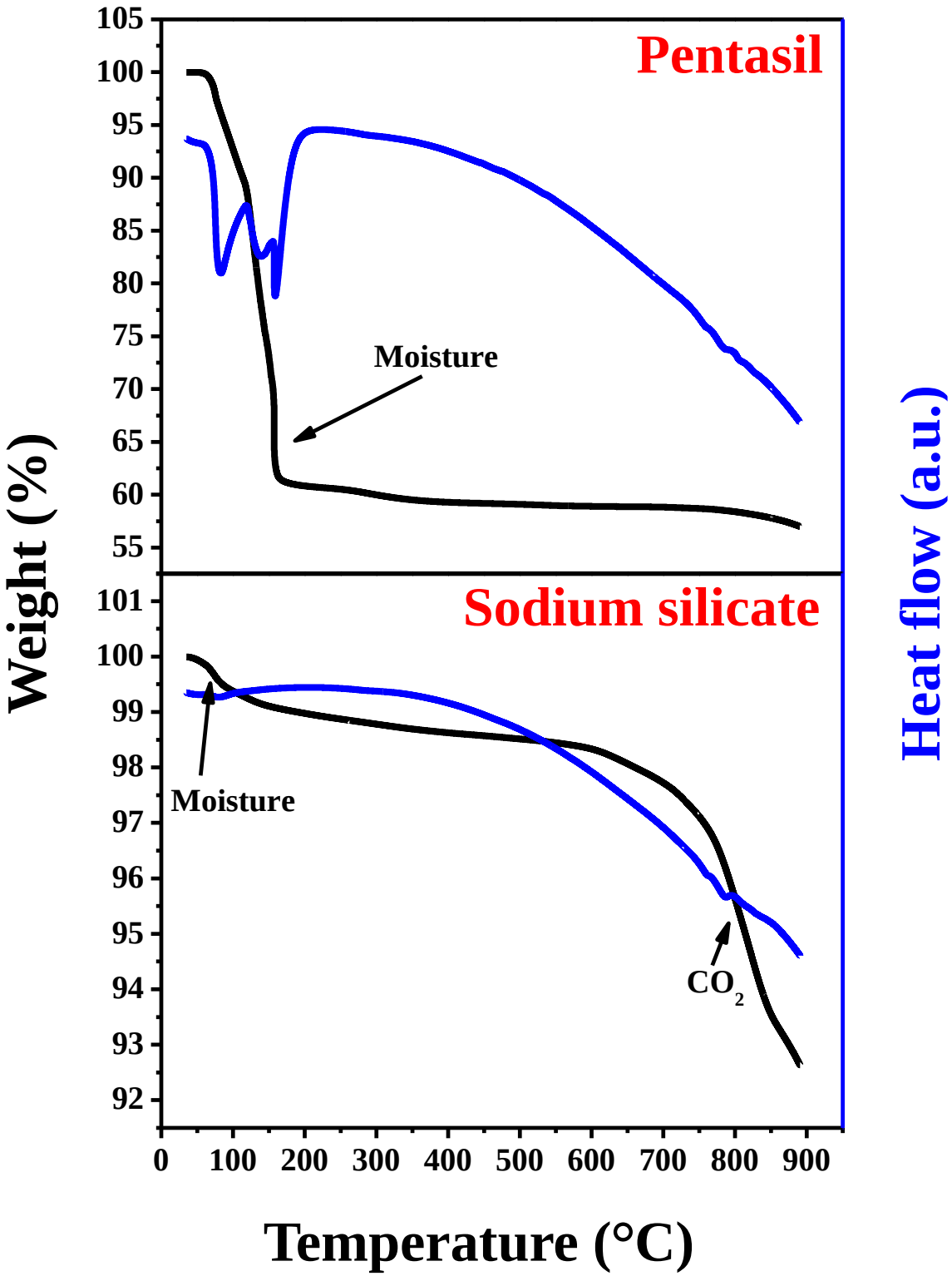

Figure 5 (continued). Thermal analyses of the raw materials by TGA/DSC (continued on next page).

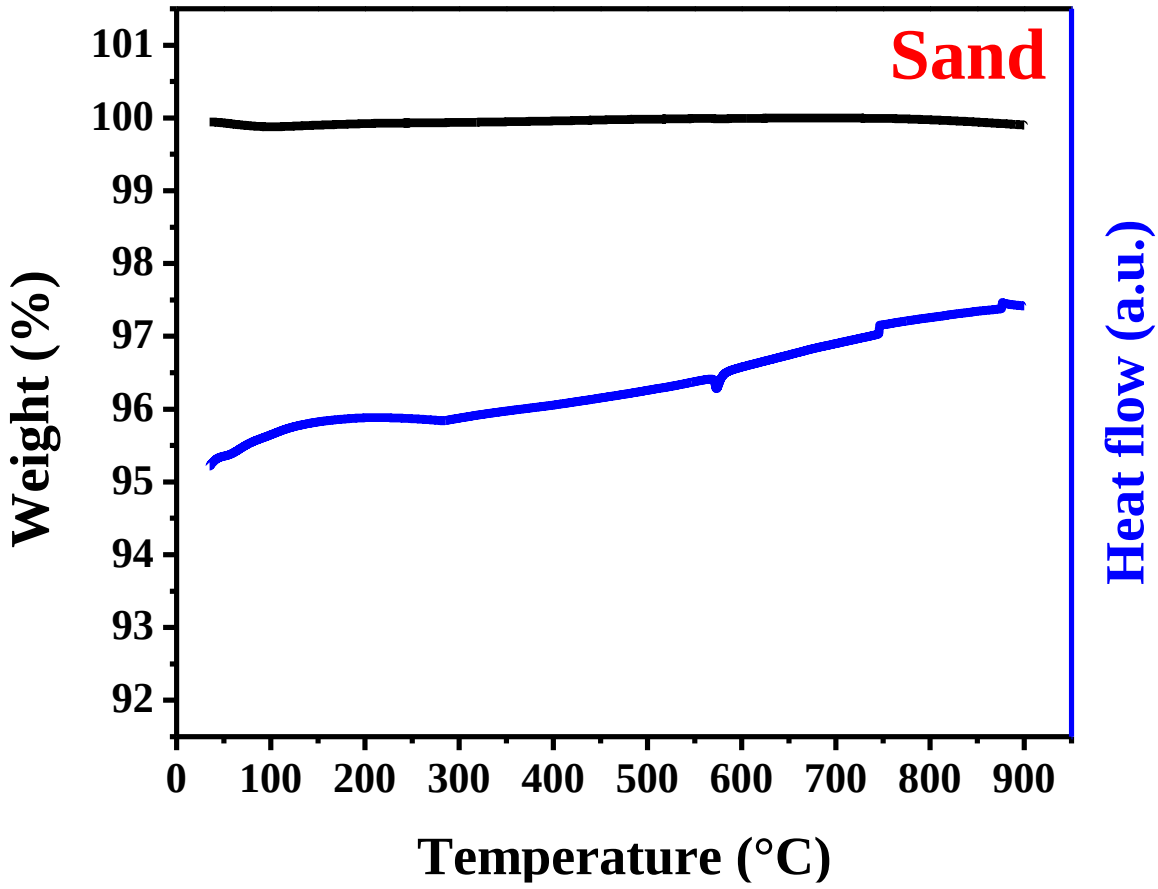

Figure 5 (continued). Thermal analyses of the raw materials by TGA/DSC.

3.1.4 Fourier transform infrared spectroscopy.

FTIR spectra of the raw materials are presented in Figure 6. The asymmetric stretching vibration of Si–O–T linkages, where T could be Si or Al, corresponds to the region between 1300 and 900 cm^{-1} [20]. The bands at 1169 and 1063 cm^{-1} are associated to the asymmetric stretching mode of the materials [20]. The bands at 1445 cm^{-1} are assumed to be a presence of carbonates [16]. A band at 1204 cm^{-1} is considered to be a stretching vibration of terminal Si–OH groups [20]. The band at around 790 cm^{-1} corresponds to the asymmetric tension of the linkage Si-O-Si [31]. The band at around 800 cm^{-1} is attributed to the vibrations of AlO_4 [31]. The H-O-H vibrations are presented in the region between 1640 cm^{-1} and 1660 cm^{-1} [31]. Finally, the bands located between 400 and 600 cm^{-1} are associated to the deformation vibrations of the linkage of Si-O-Si and Al-O-Si [31].

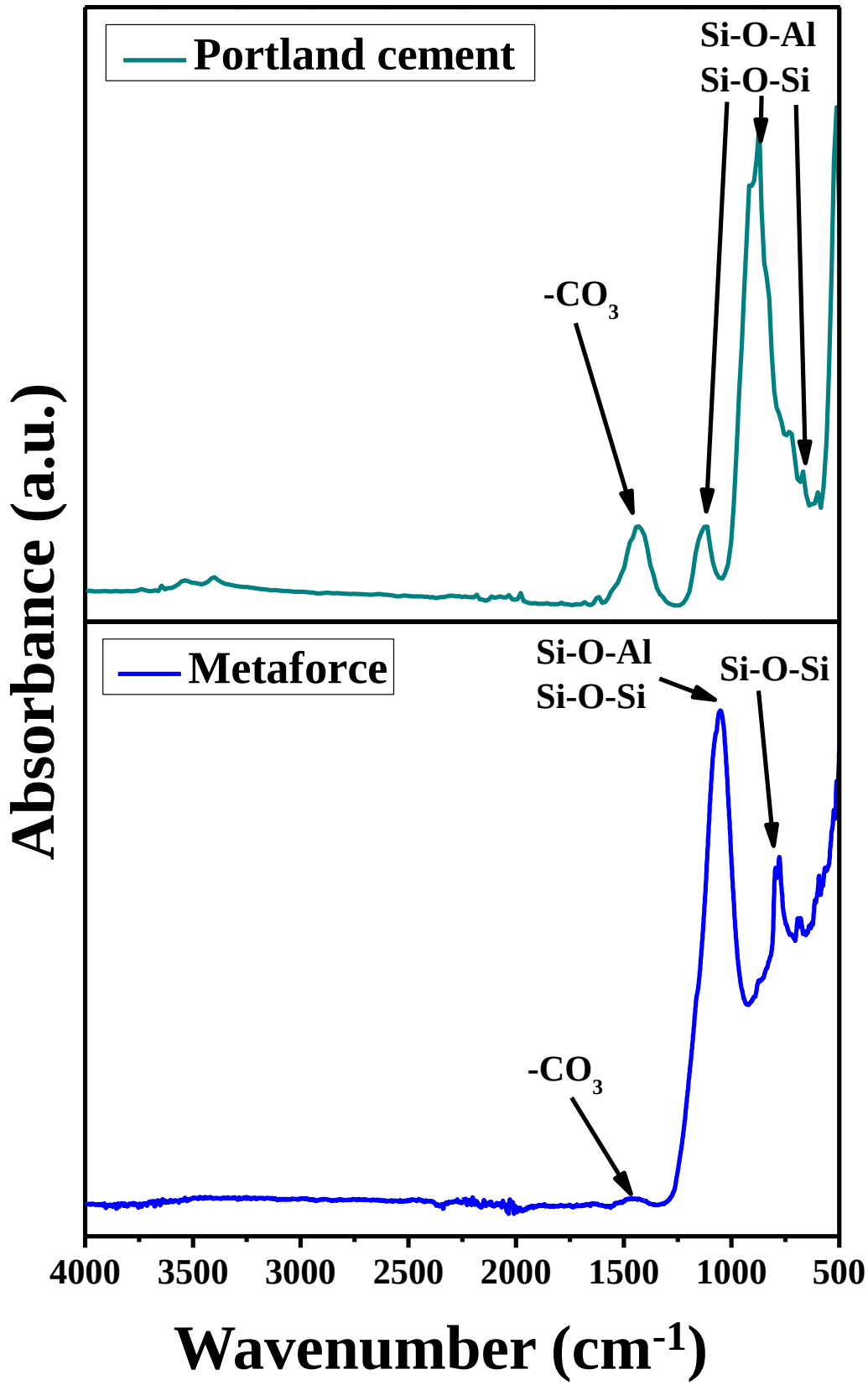

Figure 6. FTIR results of the raw materials (continued on next page).

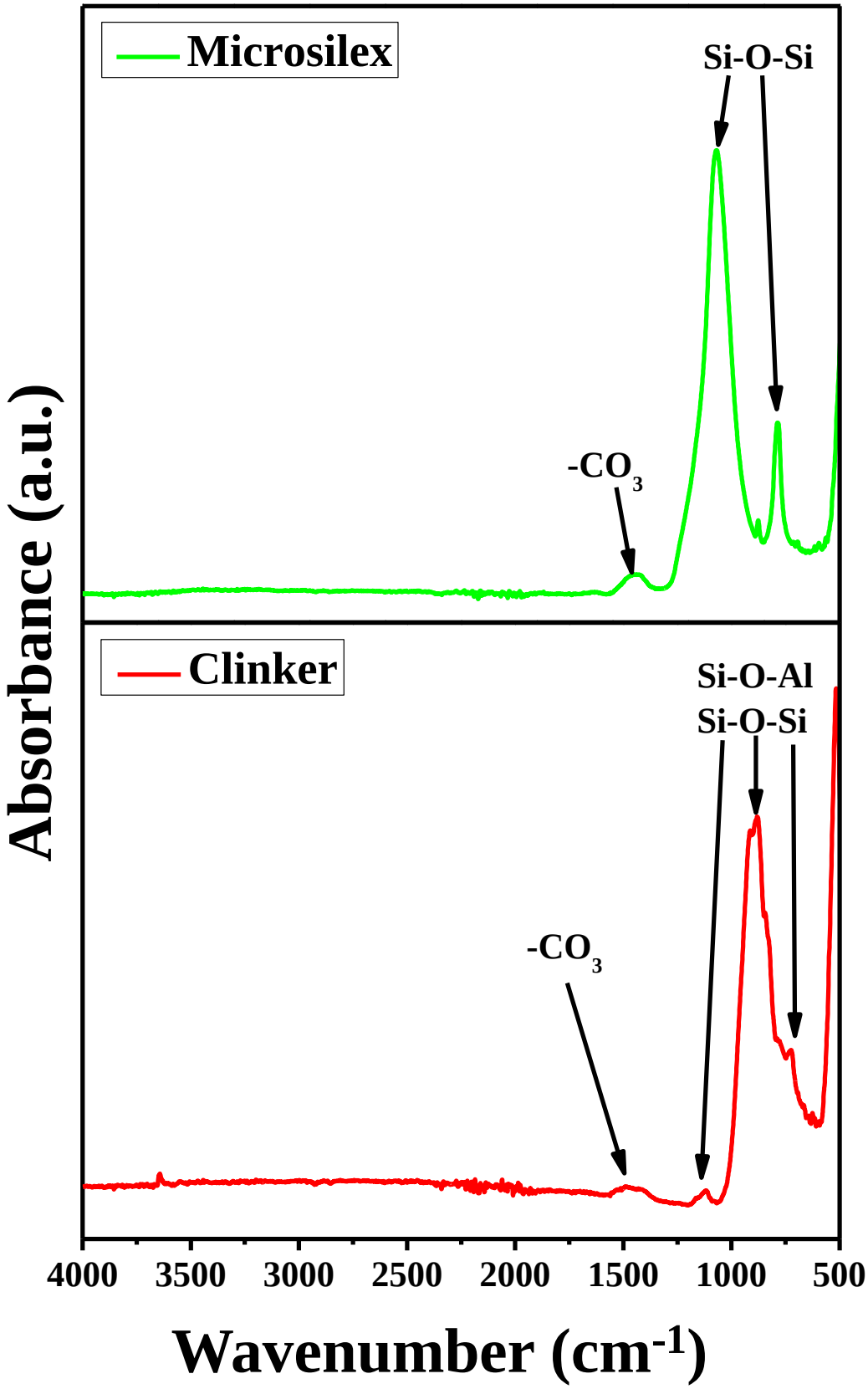

Figure 6 (continued). FTIR results of the raw materials (continued on next page).

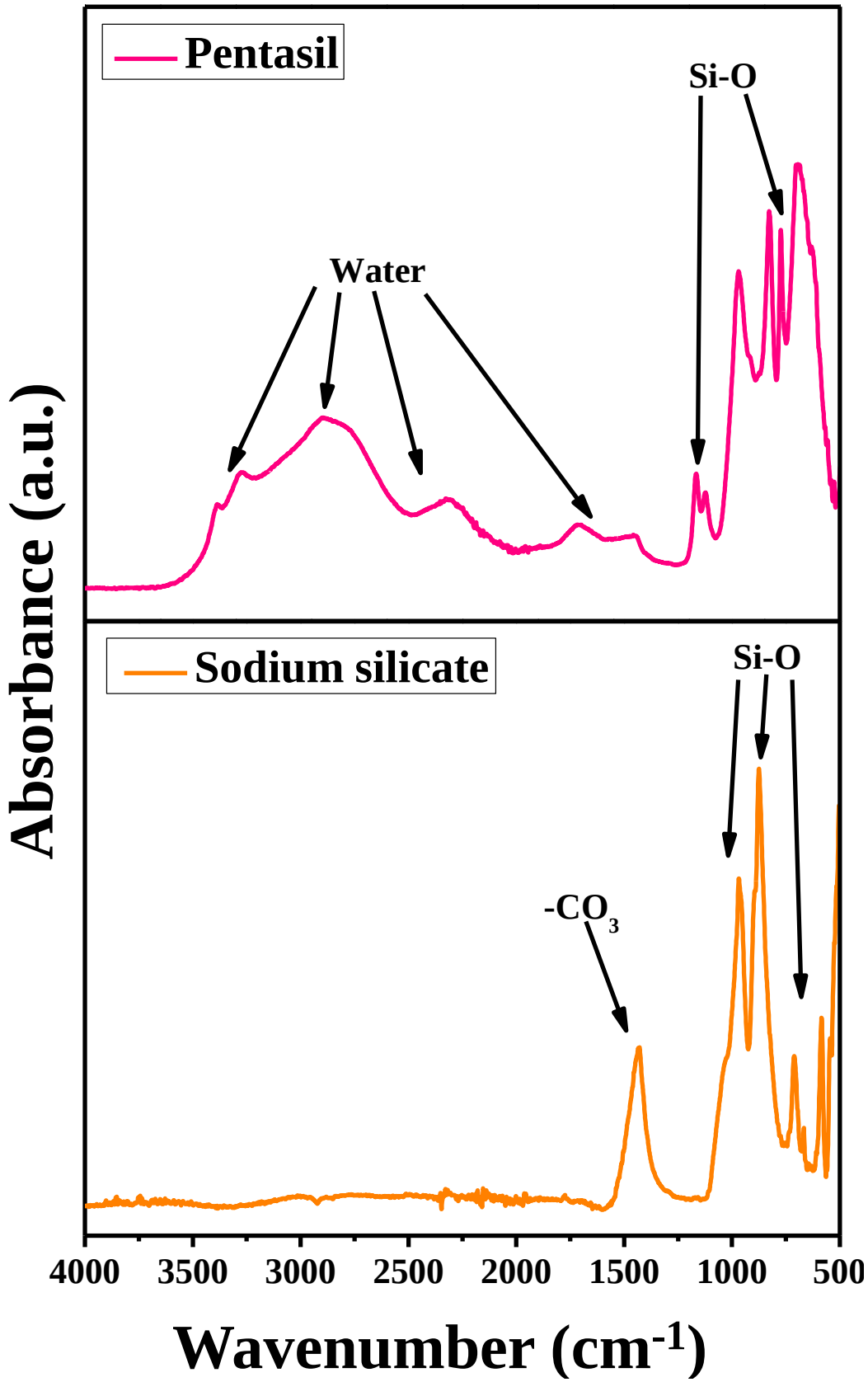

Figure 6 (continued). FTIR results of the raw materials (continued on next page).

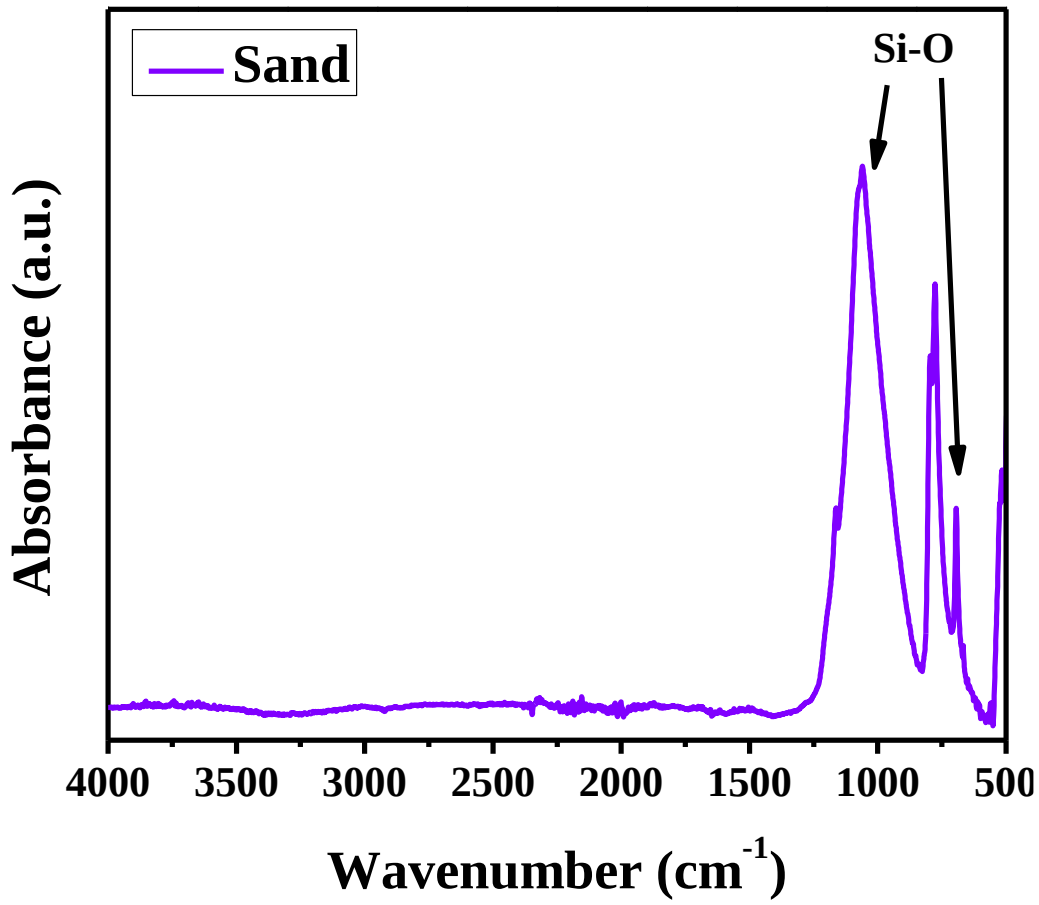

Figure 6 (continued). FTIR results of the raw materials.

3.1.5 Surface area and porosity (B.E.T.).

Figure 7 displays the results of the surface area measurement. With these results, it is possible to know the contact area that each raw material will have to produce the geopolymerization reaction. The surface area of Pentasil® could not be possible to measure since it got a chewy consistence while doing the analysis. As can be seen, Microsilex® has the highest surface area, which indicates that it has more contact area where the geopolymeric reaction can ocurre, in comparison with the others.

Activators should have a high surface area. If they do not, the geopolymeric reaction would be inefficient since the amount of activators must increase until having enough area where all the components can react.

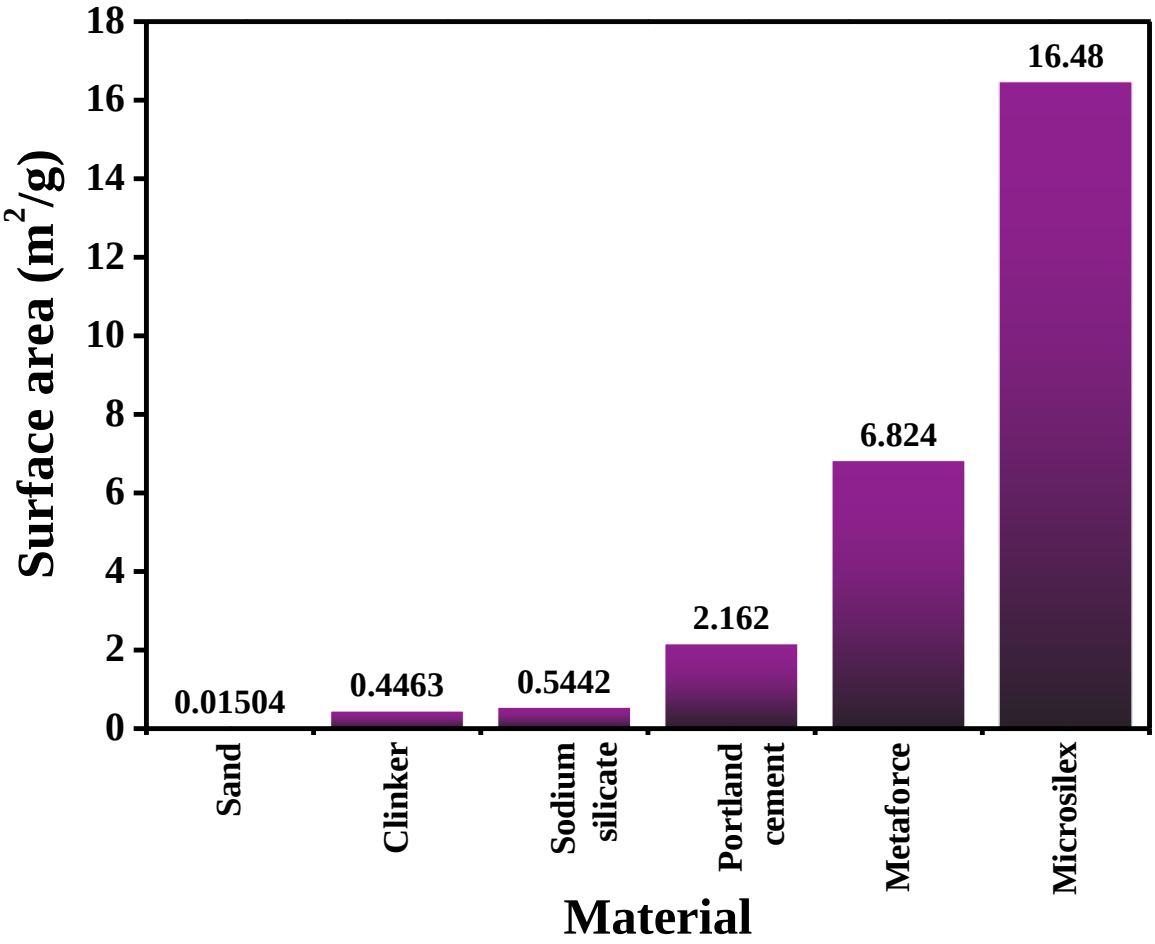

Figure 7. Surface area of the raw materials.

3.1.6 X-ray fluorescence.

Table 7 indicates the compositions in oxides of the raw materials. In general, all the raw materials have a large amount of silica; Metaforce® also contains a significant amount of alumina. The presence of calcium in clinker, detected by EDS, was verified by XRF analysis. This technique allowed to determine that the main component was calcium oxide. The composition of clinker is similar to that of the Portland cement. Microsilex® is basically a silica compound. Finally, Pentasil® and sodium silicate demonstrated to have a noteworthy amount of sodium oxide. Those considerations were taken into account for the design of the

formulations to synthesize the geopolymeric materials, since their compositions are generally expressed as $nM_2O \cdot Al_2O_3 \cdot xSiO_2 \cdot yH_2O$, where M is an alkali metal [32].

Table 7. Composition in oxides of the raw materials in wt% determined by XRF.

Material	SiO_2	Al_2O_3	Na_2O	Fe_2O_3	CaO	MgO	K_2O	SO_3
Metaforce®	55.50	30.75	0.08	1.85	6.64	0.27	0.37	0.71
Microsilex®	82.16	6.95	0.30	1.26	5.67	0.18	0.02	0.93
Clinker	21.00	4.90	0.13	3.48	66.24	2.77	0.56	0.34
Pentasil®	29.23	-	13.40	0.02	-	0.02	-	0.02
Sodium Silicate	45.89	-	23.58	0.40	0.38	0.05	1.50	0.08
Sand	93.90	2.21	-	1.14	0.37	-	0.17	0.01
Portland cement	20.05	4.73	0.30	3.07	65.52	2.21	0.12	2.89

3.1.7 X-ray diffraction.

A qualitative analysis by XRD was made in order to know the different phases contained in each raw material. Figure 8 shows the XRD patterns for each raw material. The different colors in the miller indexes (MI) indicates that the material has different phases. Some of the peaks could not be identified due to its low intensity but they are not significant because they represent a very small fraction of the pattern. Table 8 summarize the information related to the phases.

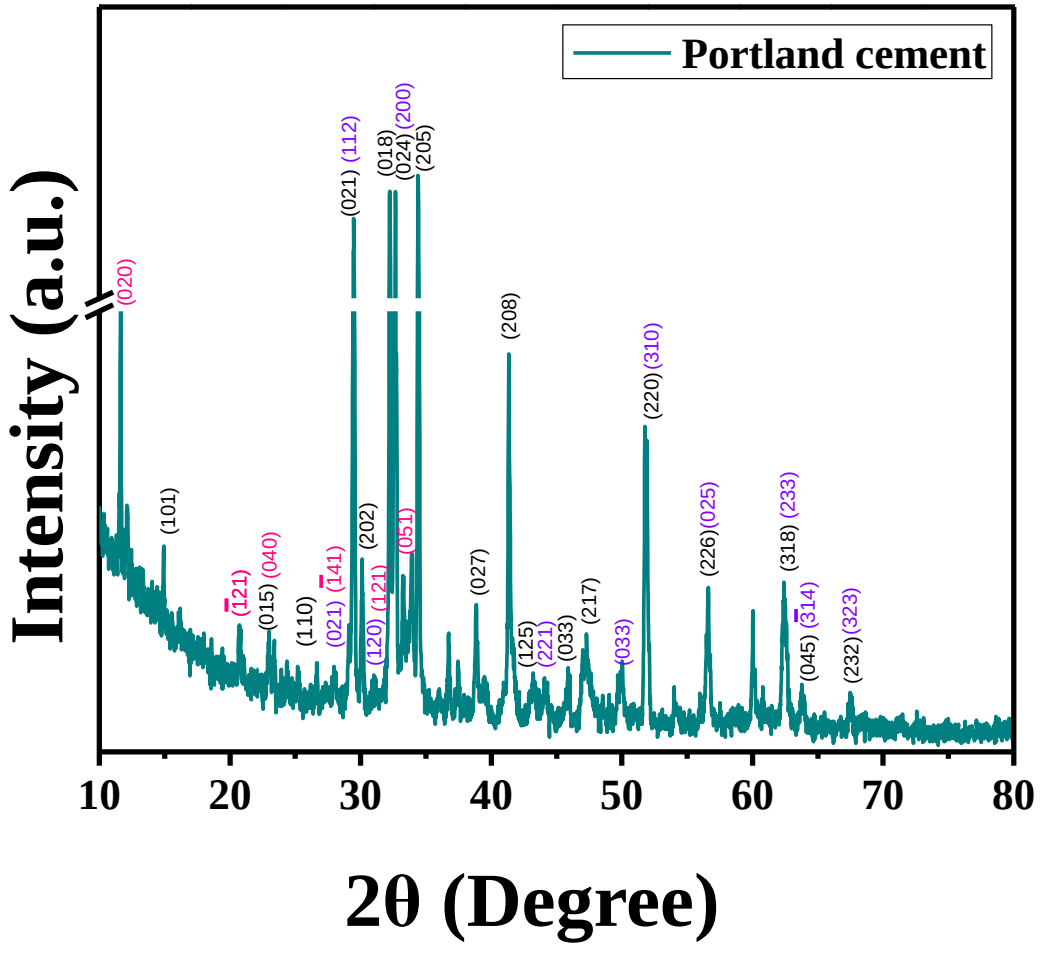

Figure 8. XRD patterns of the raw materials (continued on next page).

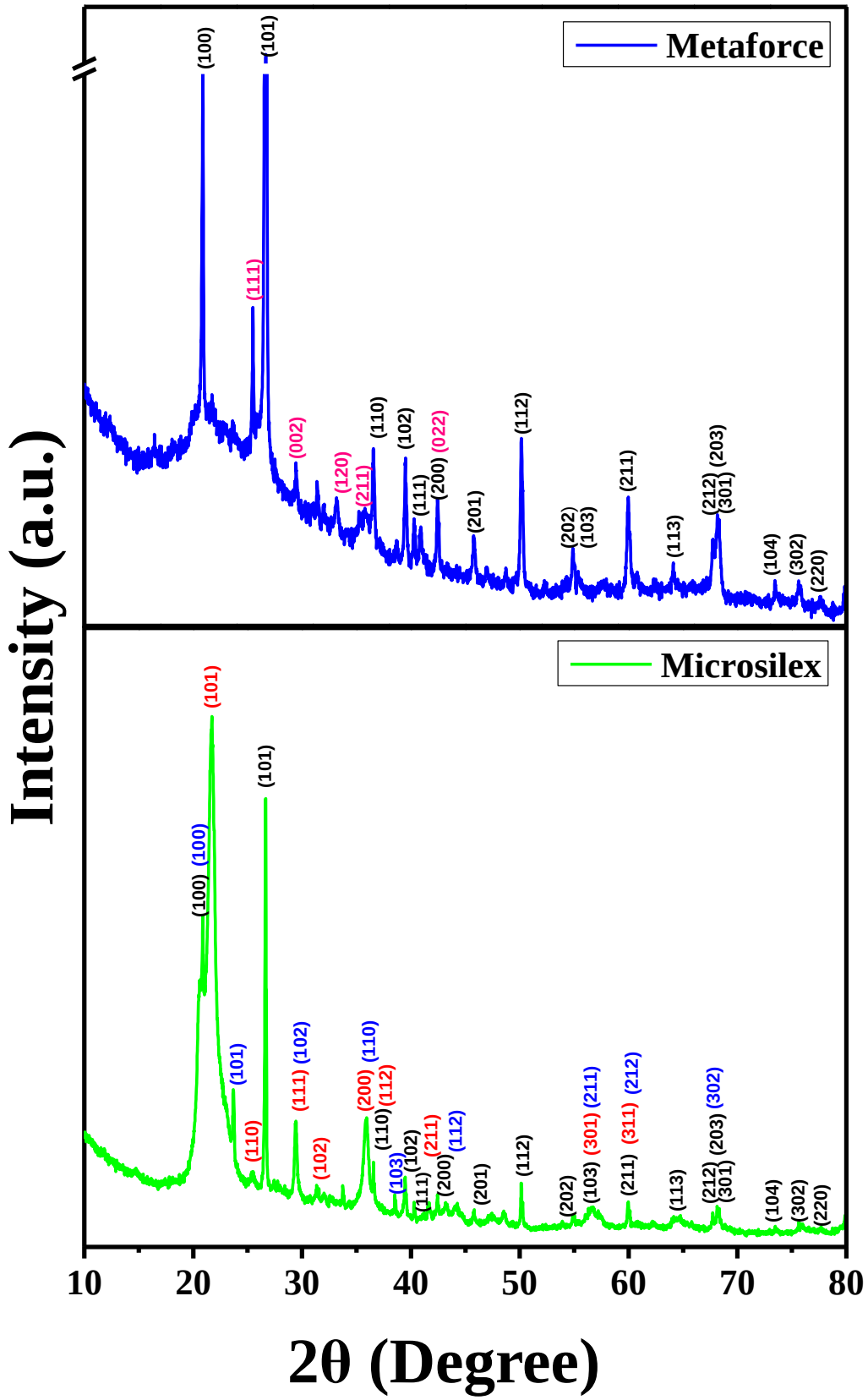

Figure 8 (continued). XRD patterns of the raw materials (continued on next page).

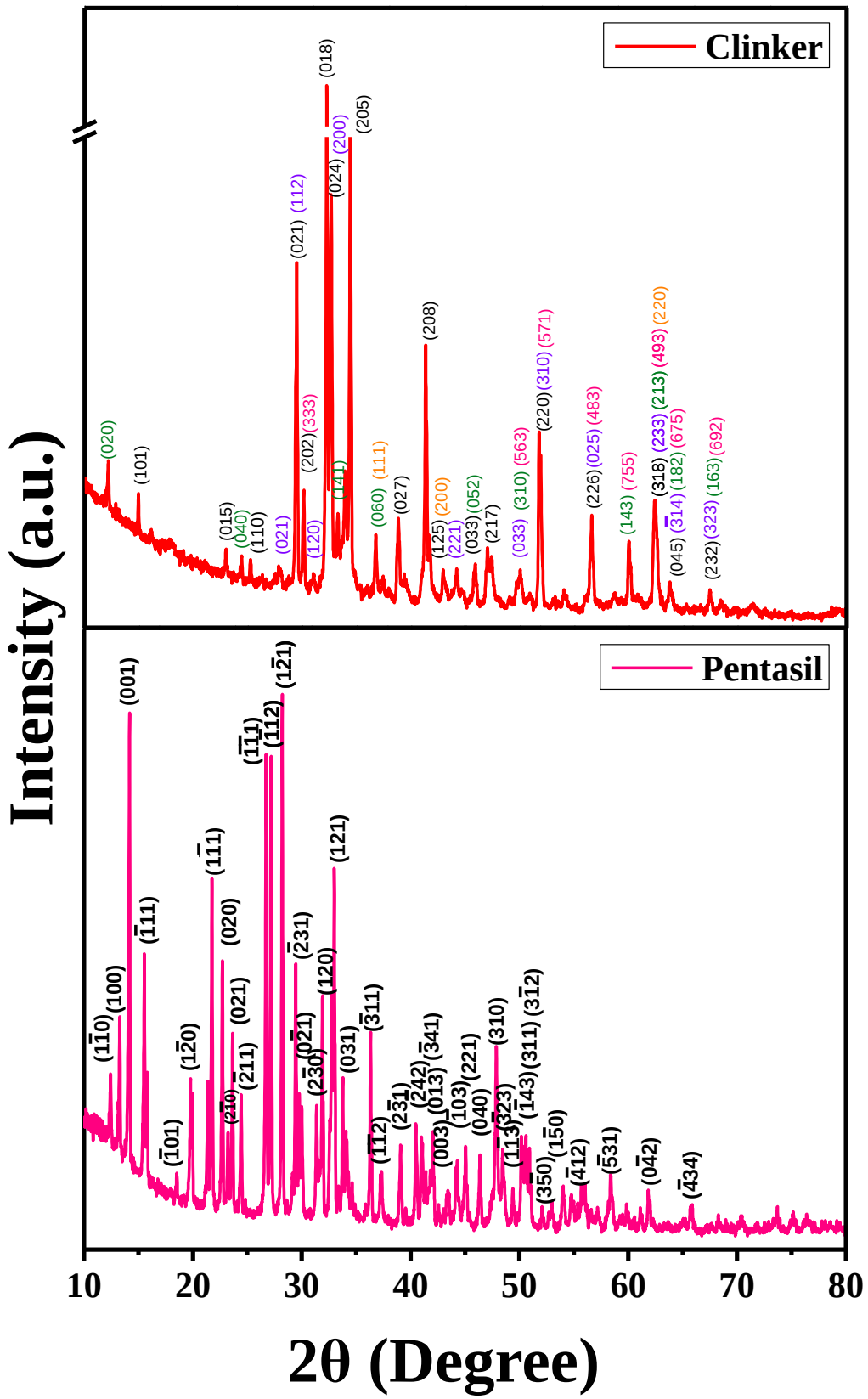

Figure 8 (continued). XRD patterns of the raw materials (continued on next page).

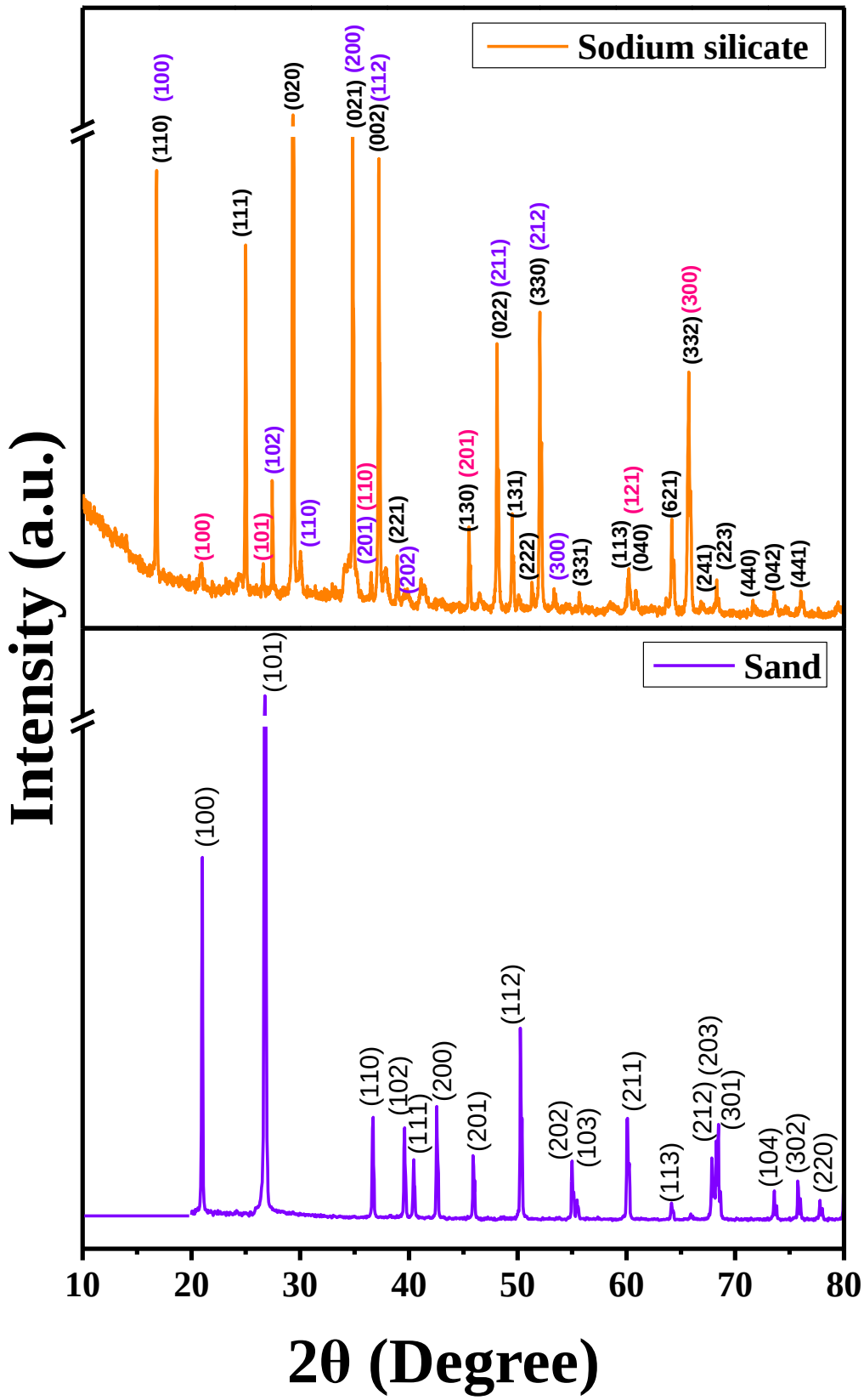

Figure 8 (continued). XRD patterns of the raw materials.

Table 8. XRD patterns information of the raw materials.

Sample	Phases	Chemical formula	Crystalline system	MI color
Portland cement	Alite	$3CaO{\cdot}SiO_2$	Monoclinic	Black
	Gypsum	$CaSO_4{\cdot}2H_2O$	Monoclinic	Pink
	Belite	$2CaO{\cdot}SiO_2$	Monoclinic	Violet
Metaforce®	Quartz	SiO_2	Trigonal	Black
	Sulfur dioxide	SO_2	Orthorhombic	Red
Microsilex®	Quartz	SiO_2	Trigonal	Black
	Cristobalite	SiO_2	Tetragonal	Red
	Tridymite	SiO_2	Hexagonal	Blue
Clinker	Alite	$3CaO{\cdot}SiO_2$	Monoclinic	Black
	Belite	$2CaO{\cdot}SiO_2$	Monoclinic	Violet
	Ferrite	$4CaO.Al0_3.Fe_2O_3$	Orthorhombic	Green
	Tricalcium aluminate	$3CaO.Al_2O_3$	Cubic (CS)	Pink
	Periclase	MgO	Cubic (FCC)	Yellow
Pentasil®	Sodium metasilicate pentahydrate	$Na_2SiO_3{\cdot}5H_2O$	Triclinic	Black
Sodium silicate	Sodium silicate	Na_2SiO_3	Orthorhombic	Black
	Quartz	SiO_2	Trigonal	Red
	Potasium sulfate	K_2SO_4	Hexagonal	Violet
Sand	Quartz	SiO_2	Trigonal	Black

3.1.8 Rietveld analyses.

A semi-quantitative analysis by XRD was made in order to know the chemical composition of the different phases contained in each raw material. Figure 9 shows the refinement made for all the raw materials through FullProf suite® software.

Metaforce® and Microsilex® contain an amorphous phase or phases. This was considered to calculate their chemical composition. A practical way to calculate the amorphous composition by the Rietveld method is adding a crystalline phase of very small crystals [27]. The amorphous content is the area between the peaks and the background, as can be seen in Figure 10.

Most of the raw materials present two or more phases and low symmetry since they have many peaks. One of the disadvantages of those polycrystalline models is that they overlap the diffraction peaks corresponding to different families of planes. Therefore, the XRD patterns were complicated to refine because of these overlaps, the number of phases and the low symmetry.

These results demonstrated that Rietveld method is a powerful and fast tool since, being the only method which is truly phase sensitive rather than element sensitive, and it is the only technique capable of determining phase contents in studies of complex structures [24].

Table 9 summarizes the results from the Rietveld refinements.

Table 9. Rietveld analyses results of the raw materials.

Sample	Phases	Chemical formula	Crystalline system	wt%
Portland cement	Alite	$3CaO \cdot SiO_2$	Monoclinic	94
	Gypsum	$CaSO_4 \cdot 2H_2O$	Monoclinic	4
	Belite	$2CaO \cdot SiO_2$	Monoclinic	2
Metaforce®	Quartz	SiO_2	Trigonal	54
	Sulfur dioxide	SO_2	Orthorhombic	2
	Amorphous			44
Microsilex®	Quartz	SiO_2	Trigonal	8
	Cristobalite	SiO_2	Tetragonal	39
	Tridymite	SiO_2	Hexagonal	52
	Amorphous			1
Clinker	Alite	$3CaO \cdot SiO_2$	Monoclinic	56
	Belite	$2CaO \cdot SiO_2$	Monoclinic	23
	Ferrite	$4CaO.Al0_3.Fe_2O_3$	Orthorhombic	16
	Tricalcium aluminate	$3CaO.Al_2O_3$	Cubic (CS)	3
	Periclase	MgO	Cubic (FCC)	2
Pentasil®	Sodium metasilicate pentahydrate	$Na_2SiO_3 \cdot 5H_2O$	Triclinic	100
Sodium silicate	Sodium silicate	Na_2SiO_3	Orthorhombic	52
	Quartz	SiO_2	Trigonal	41
	Potasium sulfate	K_2SO_4	Hexagonal	7
Sand	Quartz	SiO_2	Trigonal	100

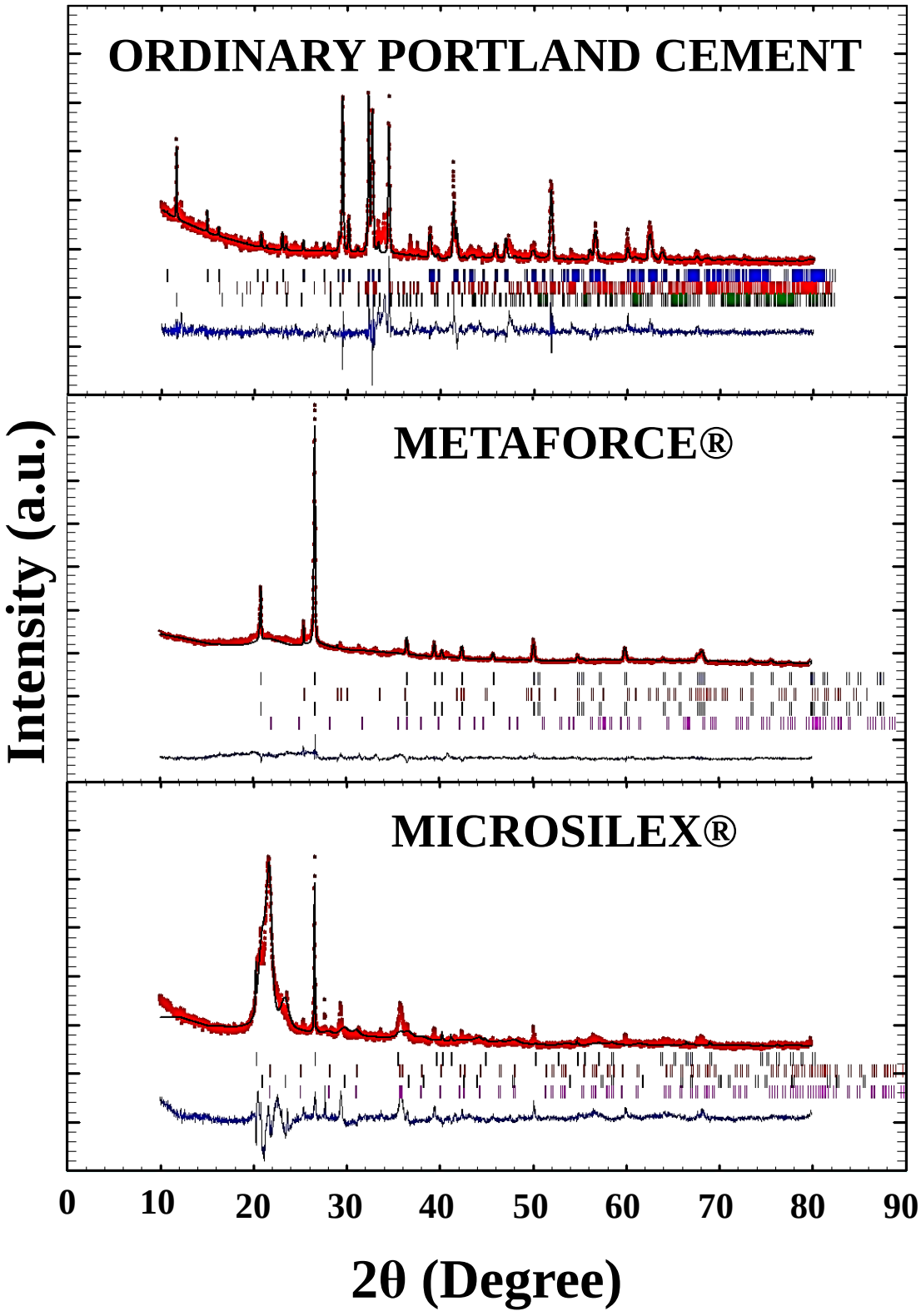

Figure 9. Rietveld refinement of the raw materials (continued on next page).

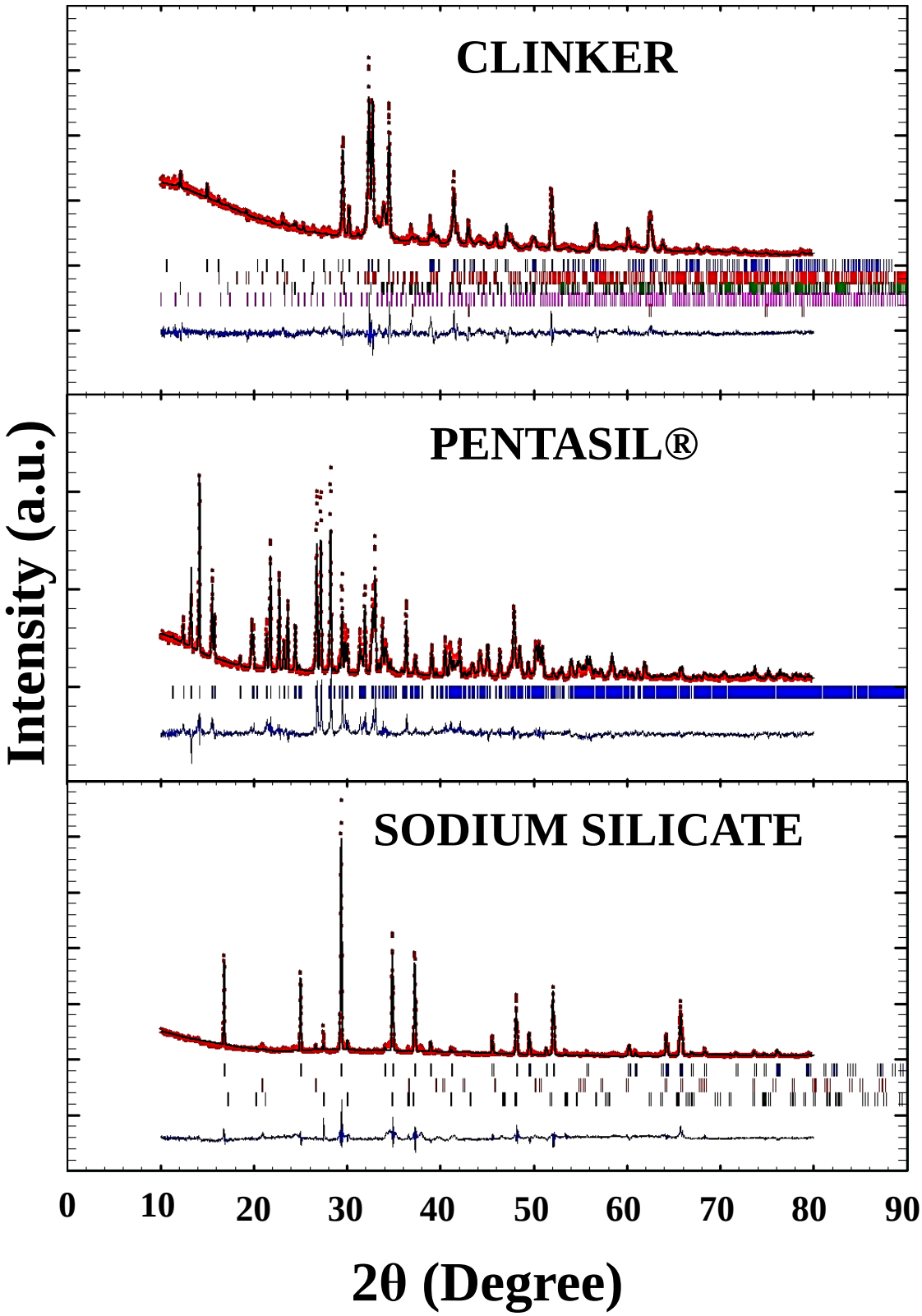

Figure 9 (continued). Rietveld refinement of the raw materials (continued on next page).

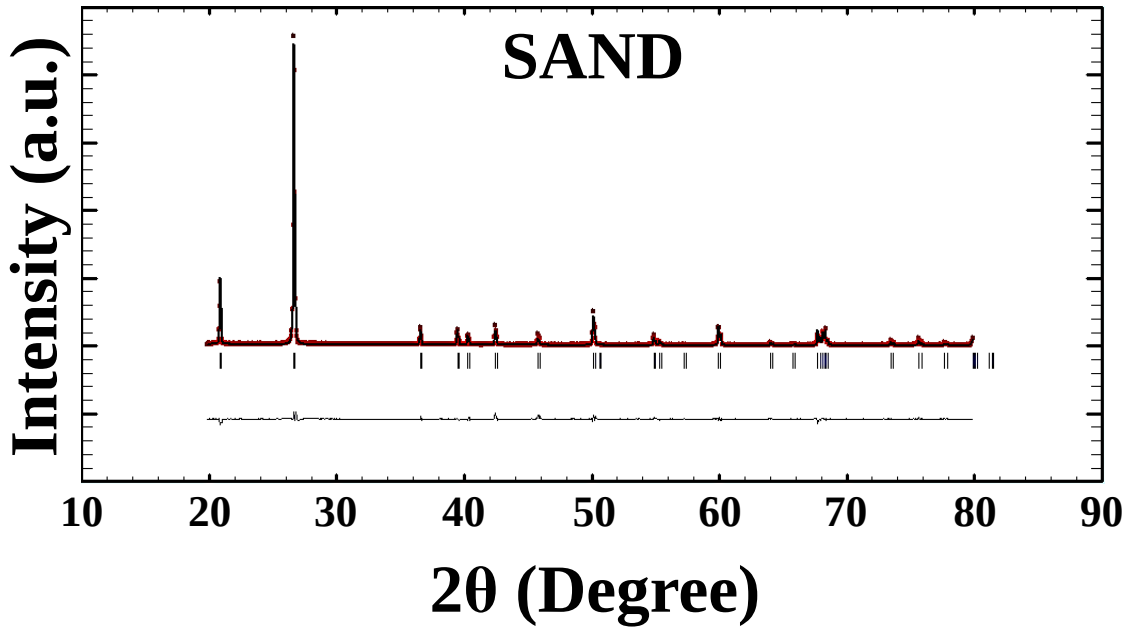

Figure 9 (continued). Rietveld refinement of the raw materials.

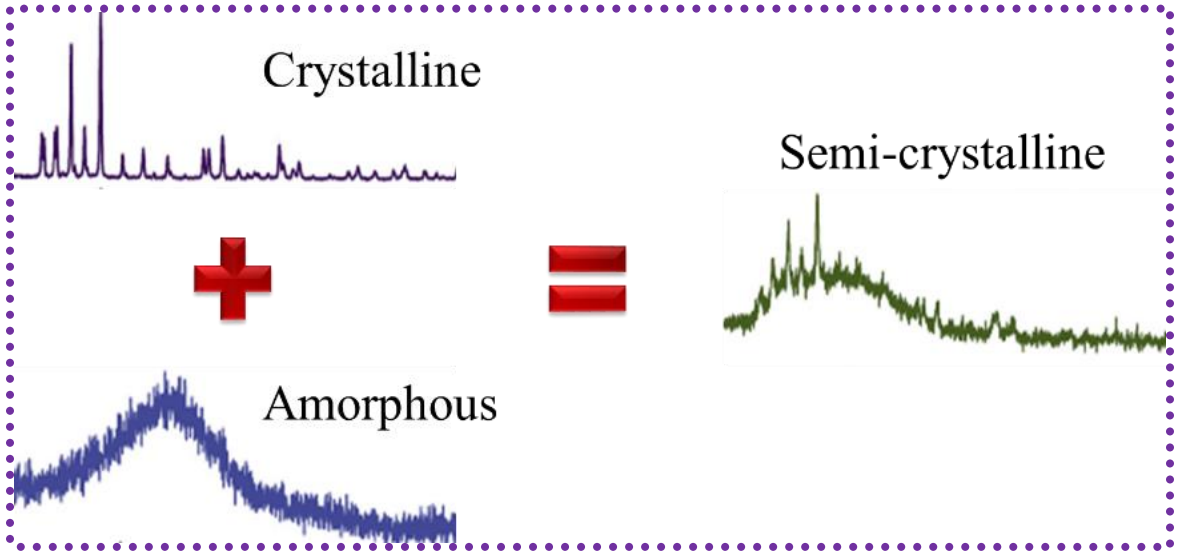

Figure 10. Semi-crystalline patterns.

3.2 Geopolymeric and ordinary pastes.

3.2.1 Compressive strength.

Figure 11 shows the compression tests results of ordinary and geopolymeric pastes after 7, 14 and 28 days of curing. As was mentioned before in the results of thermal analysis, the Portland cement used for this research work is a special cement, since its amount of calcium carbonate is low. Wang and co-workers reported that the compressive strength of the ordinary materials increases with decreasing the amount of calcium carbonate in Portland cement [33]. Therefore, the Portland cement used in this work is used for constructions that require a very high resistance under compressive loads (e.g. bridges or buildings). In general, the results of all the pastes demonstrate that there was no significant improvement of the compressive strength of geopolymeric pastes in comparison with the ordinary ones.

Formulation 1 got the highest compressive strength of all the materials synthesized for this research work, having a performance similar to the ordinary material. Then, it is possible to use it for the constructions mentioned above. Formulations 2 and 3 of geopolymers could be used for the construction of a room or a sidewalk, since their compressive strengths were not as high as the corresponding ordinary pastes, but neither as low as formulation 4. The formulation 4 was made according to the molar ratios that Barbosa and co-workers used for their experiment [29]. They report that the formulation with the molar ratios Na_2O/SiO_2 = 0.25, H_2O/Na_2O = 10.0 and SiO_2/Al_2O_3 = 3.3 had the highest compressive strength of 52 MPa after 24 h of aging. In this research work, it is clear that the formulation 4 did not work due to the pastes were crumbled and felt fragile. It was not possible to reach the results that report Barbosa and co-workers since the raw materials employed were different, the heat treatment was not performed in this work and there was no calcium-rich component that allowed increasing the mechanical properties.

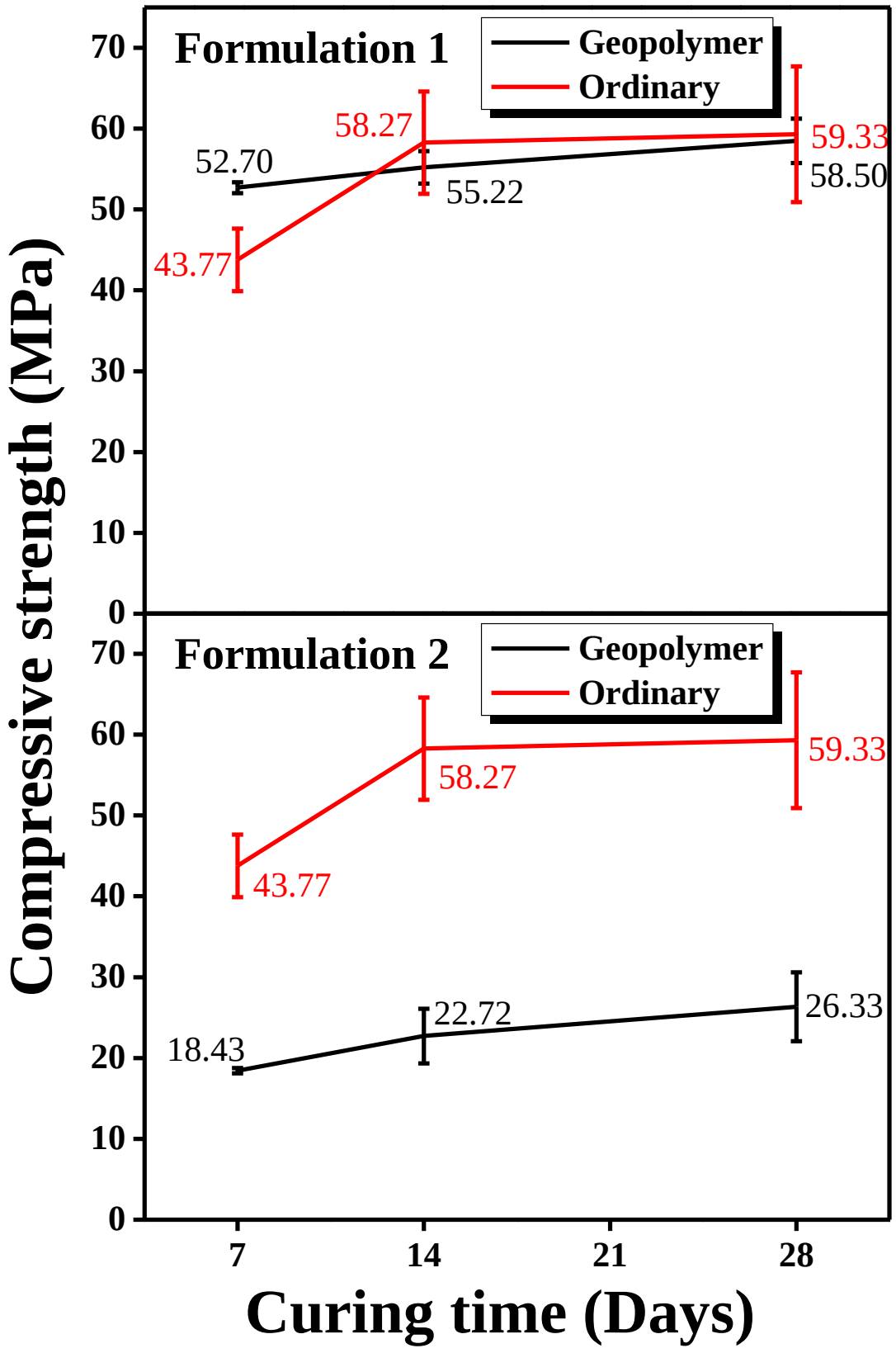

Figure 11. Compressive strength of the geopolymeric and ordinary pastes (continued on next page).

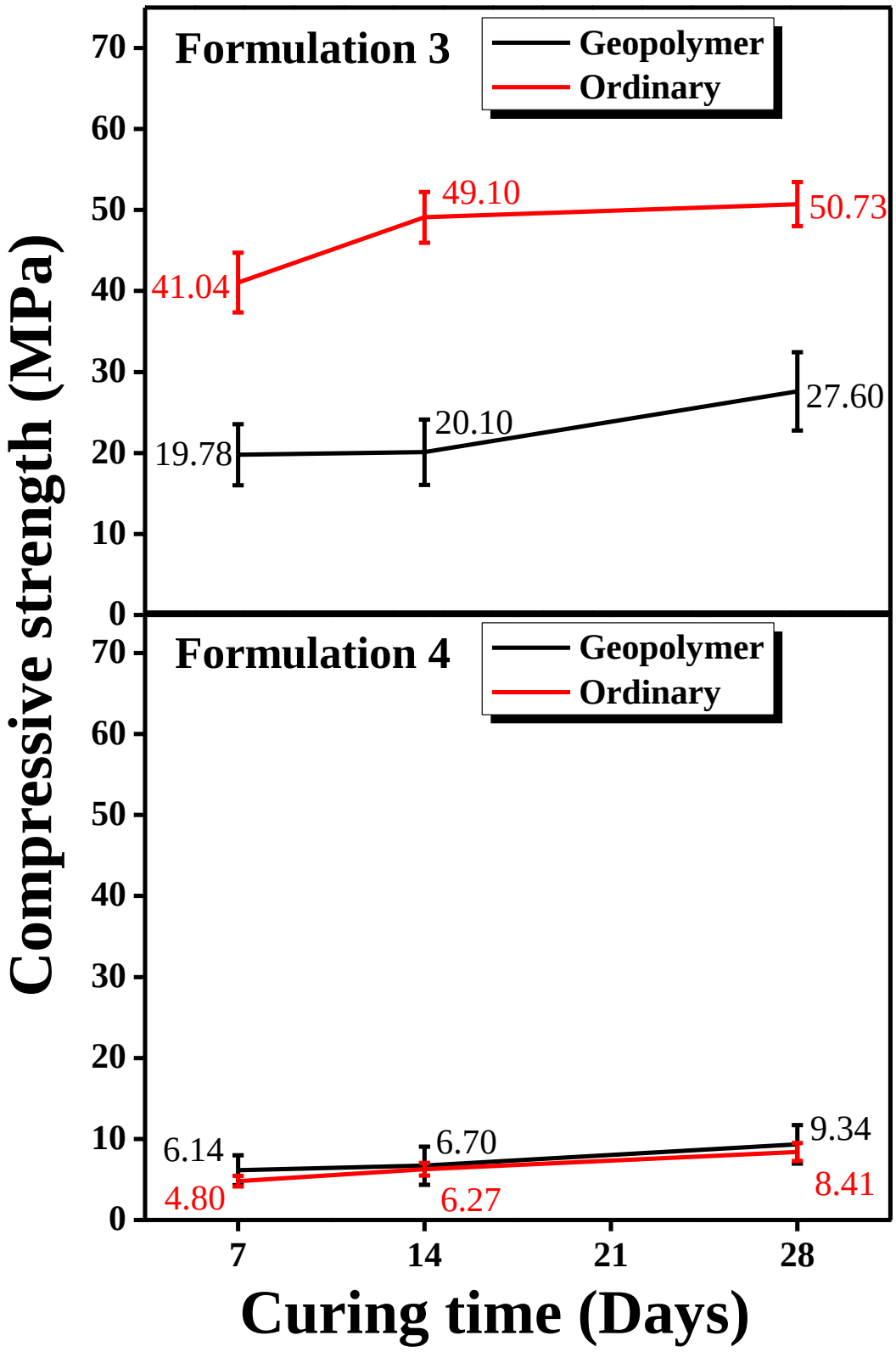

Figure 11 (continued). Compressive strength of the geopolymeric and ordinary pastes.

3.2.1.1 Effect of the particle size of clinker on the compressive strength.

Physical parameters such as particle size distribution, uniformity of the distribution and specific surface area are very important for cement strength development. Particular size fractions affect strength differently, particularly the fine and coarse tails of the distribution. Fineness is very important, especially for early strength. Same strength values could be obtained for samples with a narrower distribution but smaller specific surface area [34].

Figure 12 shows the compressive strength of the geopolymeric pastes after 7, 14 and 28 days of curing by reducing the clinker particle size to 15 and 130 µm.

The paste of formulation 4 could not be evaluated at 130 µm-particle size due to the lack of compaction of the material. Its compressive strength at 15 µm is showed in Figure 11.

As can be seen, the difference between 15 and 130 µm of clinker particle size is significant on the compressive strength results due to the surface area. The larger the particle size is, the smaller the surface area will be. The surface area is where the geopolymerization will be carried out.

That phenomena can be explained as follows: small crystals act as nucleation centers, decreasing the induction period. Therefore, the high-surface area solid particles provide nucleating sites [35]. The nucleating site is where the reaction will begin and get harden [36]. Consequently, while having more nucleating sites, it will get more harden.

Parrott and Killoh presented data indicating that the rate of hydration was proportional to the specific surface area during the period of hydration in which the rate was controlled by nucleation and growth, but not subsequently, when it was controlled by diffusion [37].

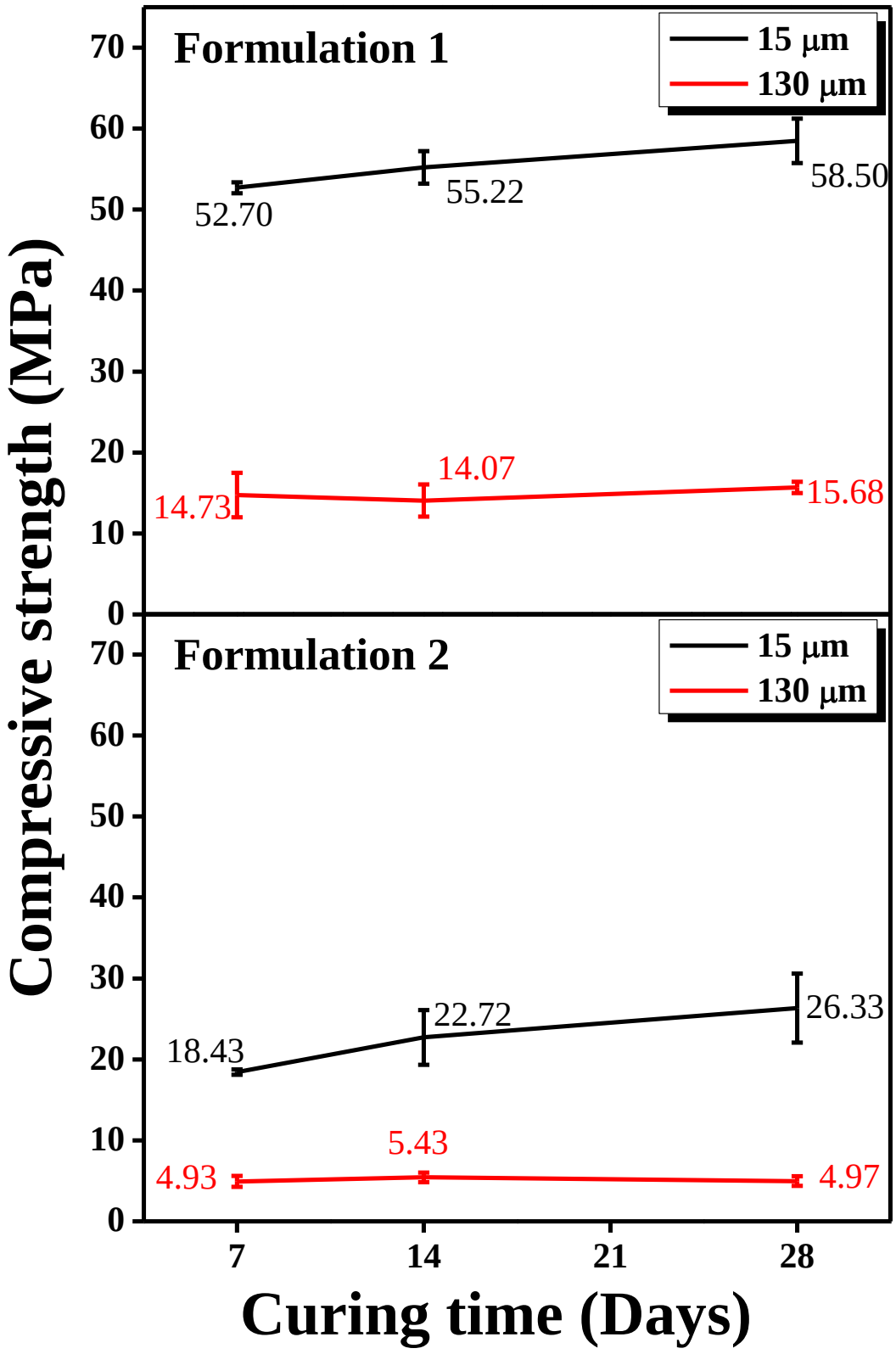

Figure 12. Compressive strength by reducing clinker particle size to 15 and 130 µm of the pastes (continued on next page).

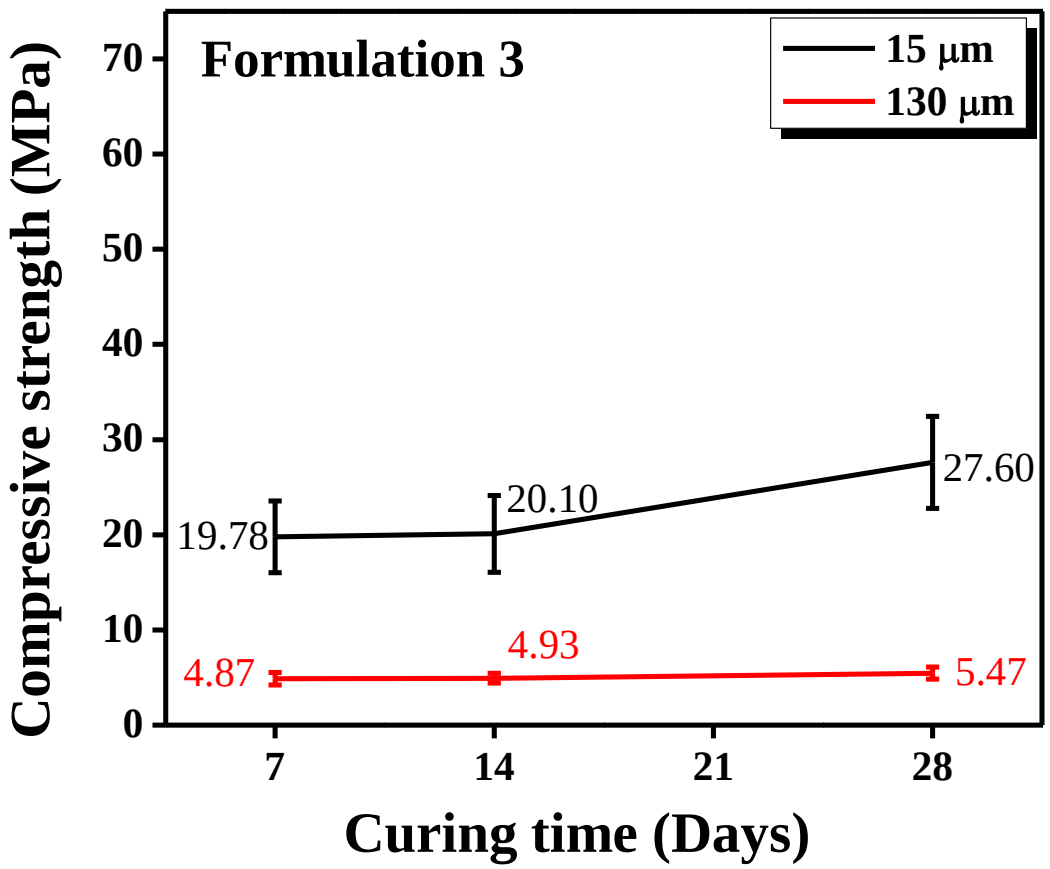

Figure 12 (continued). Compressive strength by reducing clinker particle size to 15 and 130 µm of the pastes.

3.2.1.2 Effect of dissolving the Pentasil® and/or sodium silicate in water on the compressive strength.

Figure 13 shows the compressive strength of the geopolymeric pastes after 7, 14 and 28 days of curing, having the Pentasil® and sodium silicate dissolved and undissolved in water.

As said before, activators should have high surface area in order to have enough area where all the components can react. As can be seen in Figure 4 and Figure *7*, the surface area of Pentasil® and sodium silicate, respectively, is low. This low surface area was the reason to dissolve these raw materials in water, to increase their reactivity and, consequently, their compressive strength.

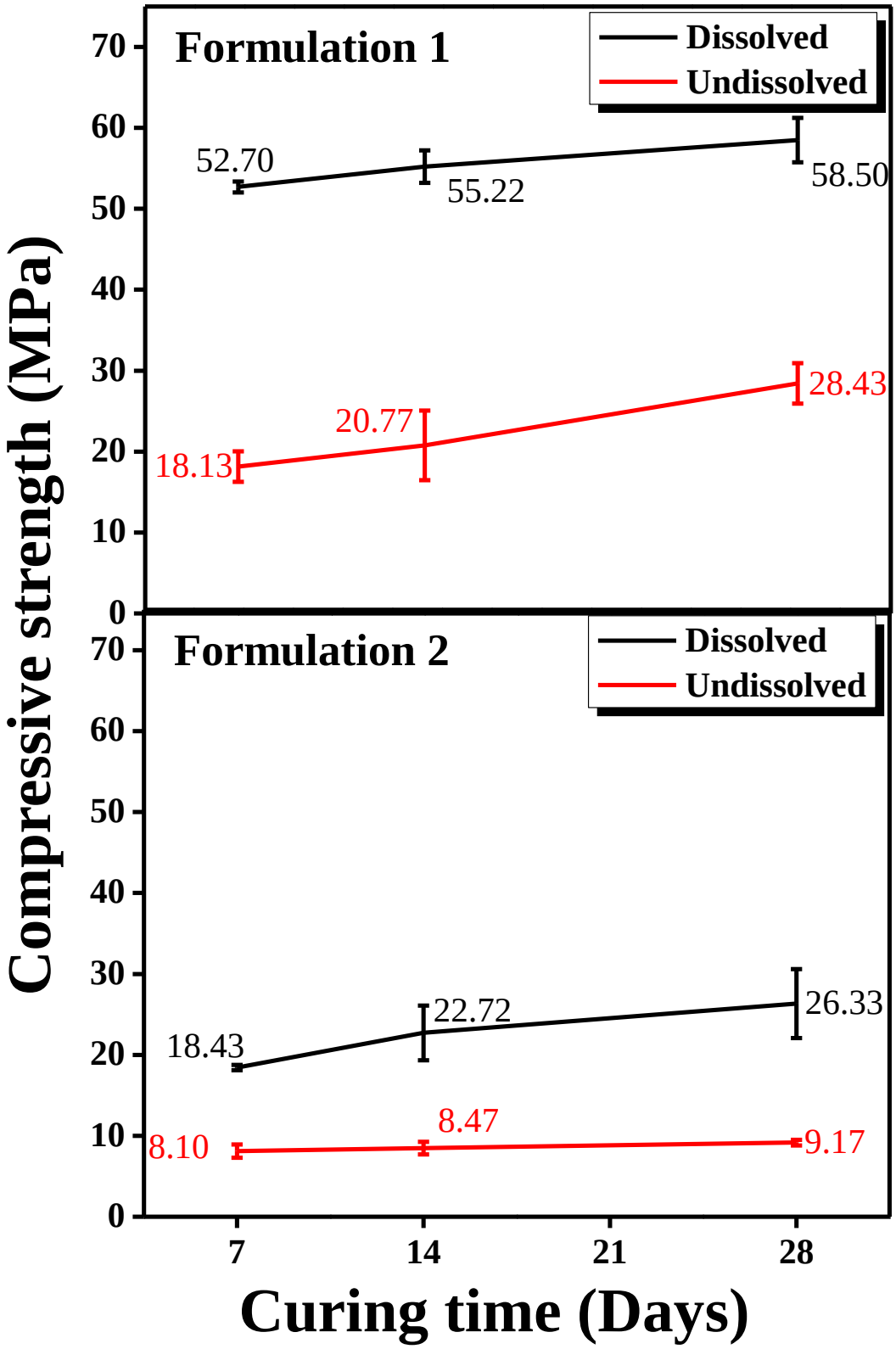

Figure 13. Compressive strength with Pentasil® and/or sodium silicate dissolved and undissolved in water of the pastes (continued on next page).

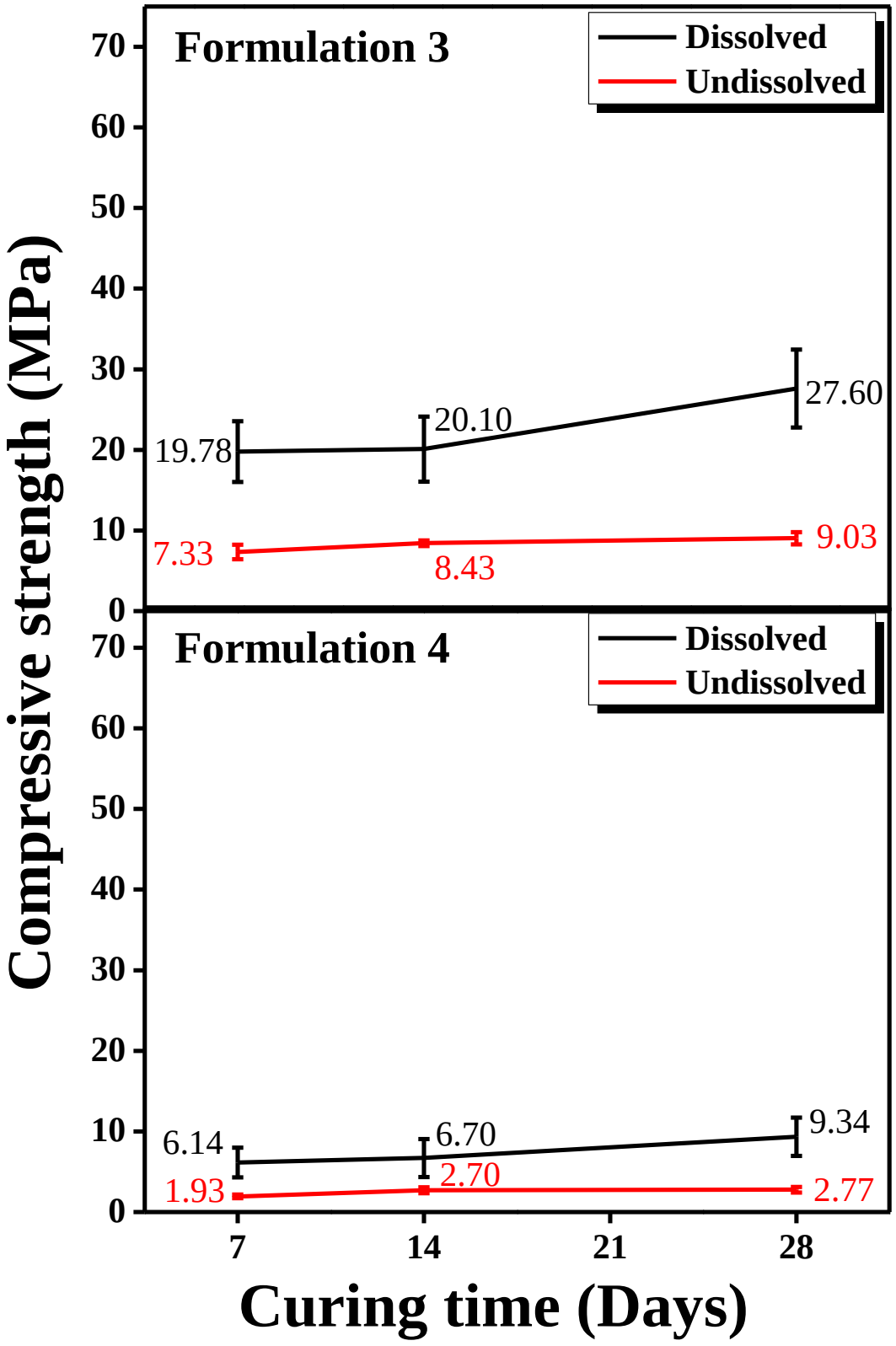

Figure 13 (continued). Compressive strength with Pentasil® and/or sodium silicate dissolved and undissolved in water of the pastes.

3.2.2 X-ray diffraction.

A qualitative XRD analysis was performed in order to know the phases presented in each geopolymeric paste. XRD patterns are illustrated in Figure 14.

The identification of phases was made by the database of X'Pert HighScore Plus software and corroborated by the FindIt software.

The results show the presence of quartz (black MI) in all the patterns and alite or tricalcium silicate (Red MI) in formulations 1, 2 and 3.

Formulation 4 does not contain alite since clinker was not used to synthesize this formulation and, as shown in Table 8, the only raw material that contain alite is the clinker, which is necessary to synthesize geopolymers. Table 10 summarize these results.

Alite has a monoclinic structure and its space group is Cm, where C means centered on the opposite face of the vector c, and m corresponds to a mirror plane.

Quartz has a trigonal structure and its space group is $P3_121$, where P corresponds to a primitive cell. This cell has three screw axes 3_1. This symmetry operation represents a rotation of $2\pi/3$ followed by a translation of 1/3 units trough the rotation axis. The number 2 represents a rotation axis of order 2.

Table 10. XRD pattern information of the geopolymeric pastes.

Formulation	Phases	Chemical formula	Crystalline system	MI color
1-3	Alite Quartz	$3CaO{\cdot}SiO_2$ SiO_2	Monoclinic Trigonal	Red Black
4	Quartz	SiO_2	Trigonal	Black

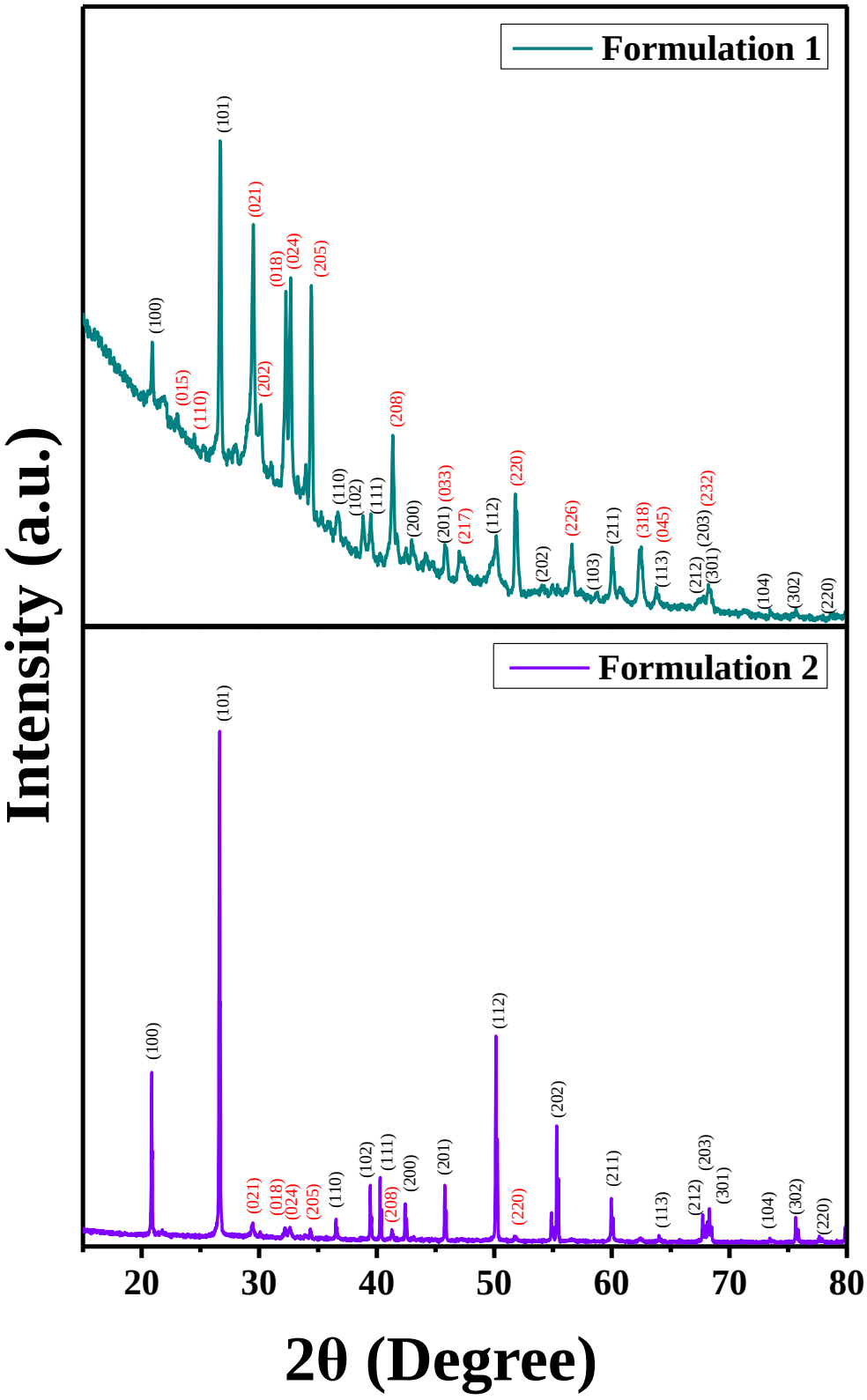

Figure 14. XRD patterns of the geopolymeric pastes (continued on next page).

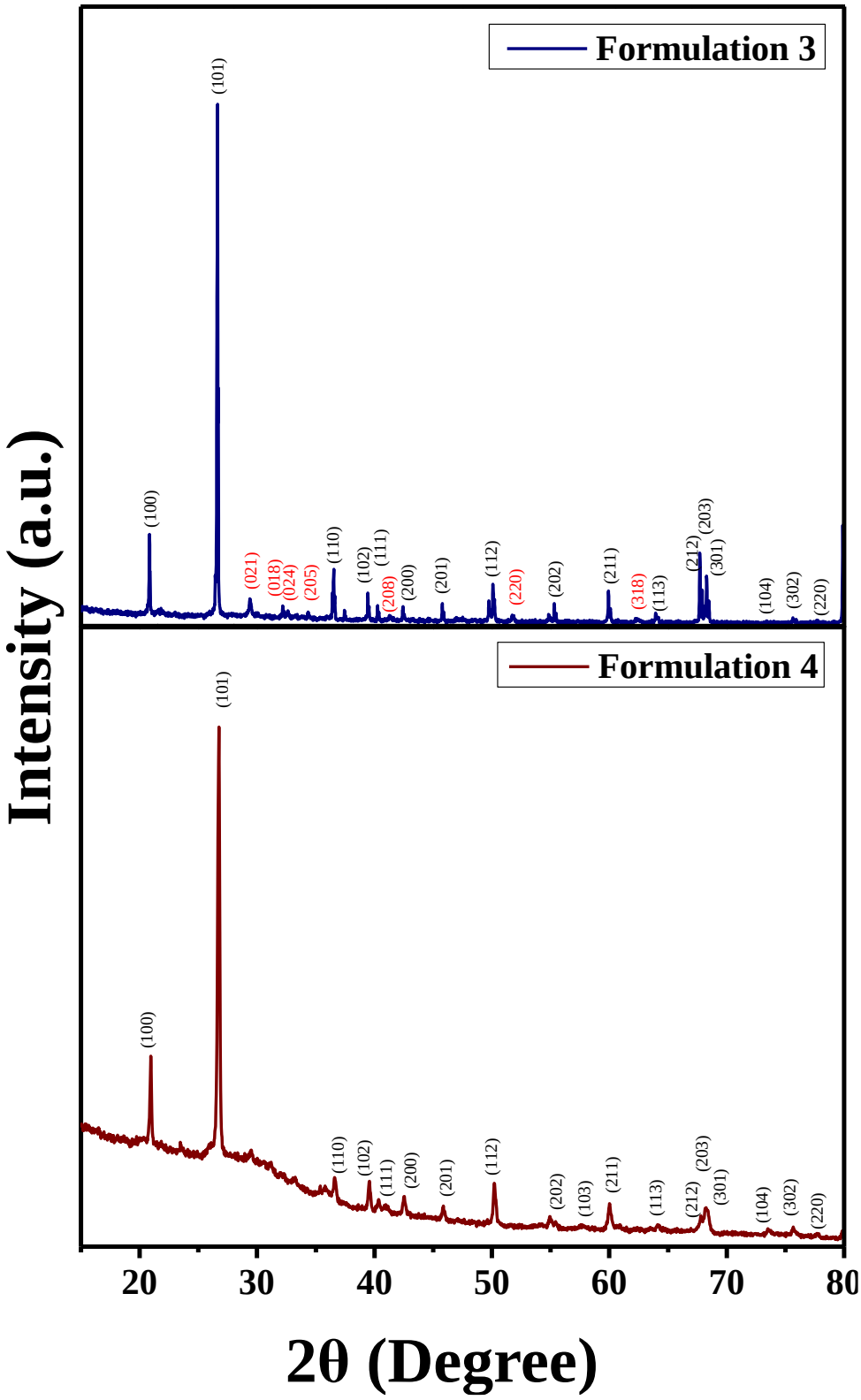

Figure 14 (continued). XRD patterns of the geopolymeric pastes.

3.2.3 Rietveld analyses.

A semi-quantitative analysis by XRD was made in order to know the chemical composition of the different phases present in the pastes. Figure 15 shows the Rietveld refinement of the pastes and Table 11 summarizes the results.

These results allowed understanding the relationship between the chemical composition of the phases present in each product and the respective compressive strength. The samples with a high content of alite demonstrate to have higher compressive strength values. These results are reasonable because the alite contributes to the development of early compressive strength of cement (generally in the first 28 days), working as a nucleating agent [38]. The amorphous phase was identified as the geopolymeric gels and calcium silicate hydrate gels [39]. It means that the geopolymeric reaction and the hydration reaction occurred at the same time, consequently it was not possible to order the atoms resulting from the amorphous phase [39].

Table 11. Rietveld analyzes results of the geopolymeric pastes.

Formulation	Phases	Chemical formula	Crystalline system	wt%
1	Alite Quartz Amorphous	$3CaO{\cdot}SiO_2$ SiO_2 -	Monoclinic Trigonal -	65 12 23
2	Quartz Alite	$3CaO{\cdot}SiO_2$ SiO_2	Monoclinic Trigonal	93 7
3	Quartz Alite	$3CaO{\cdot}SiO_2$ SiO_2	Monoclinic Trigonal	92 8
4	Quartz Amorphous	SiO_2 -	Trigonal -	67 12

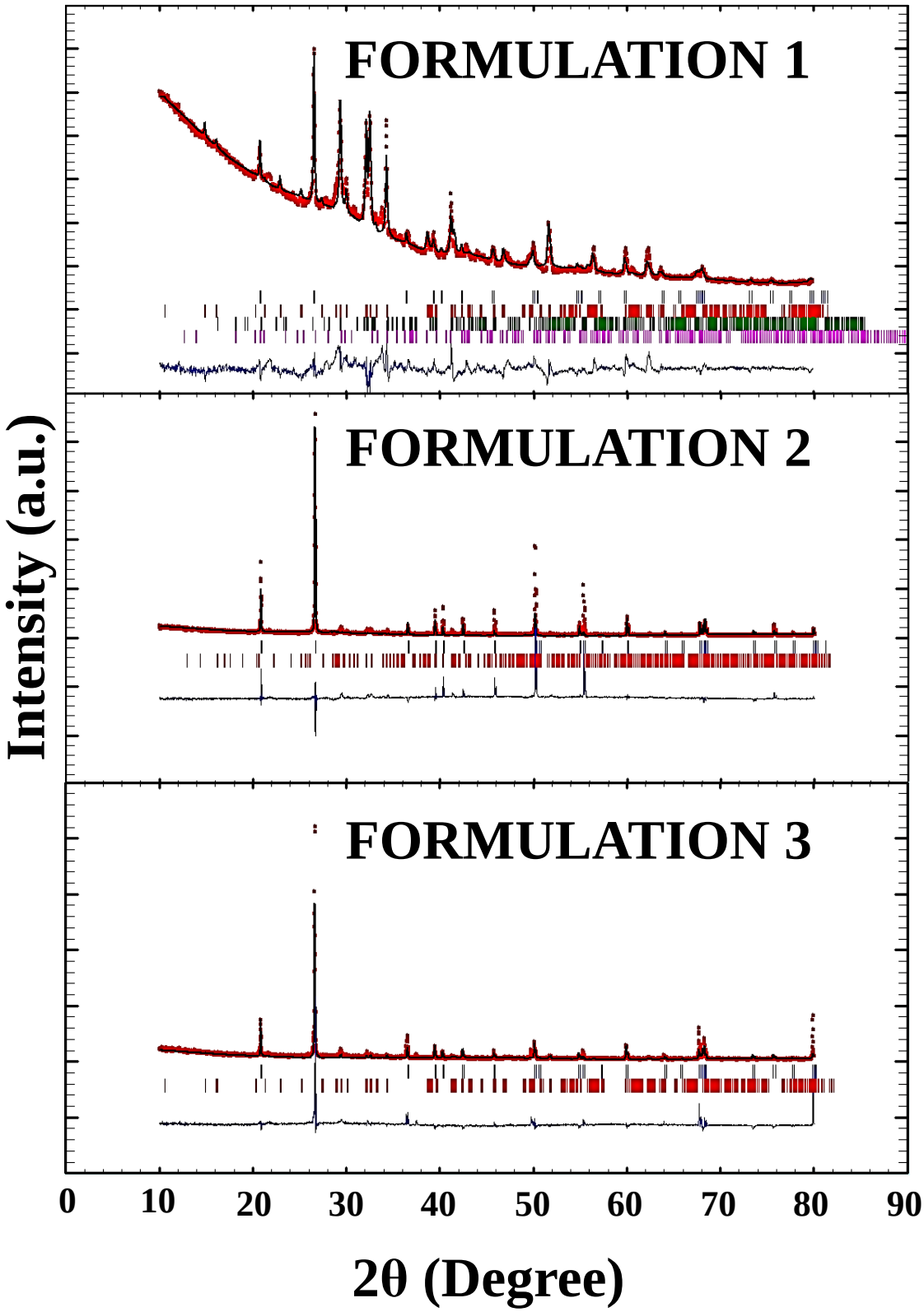

Figure 15. Rietveld refinement of the geopolymeric pastes (continued on next page).

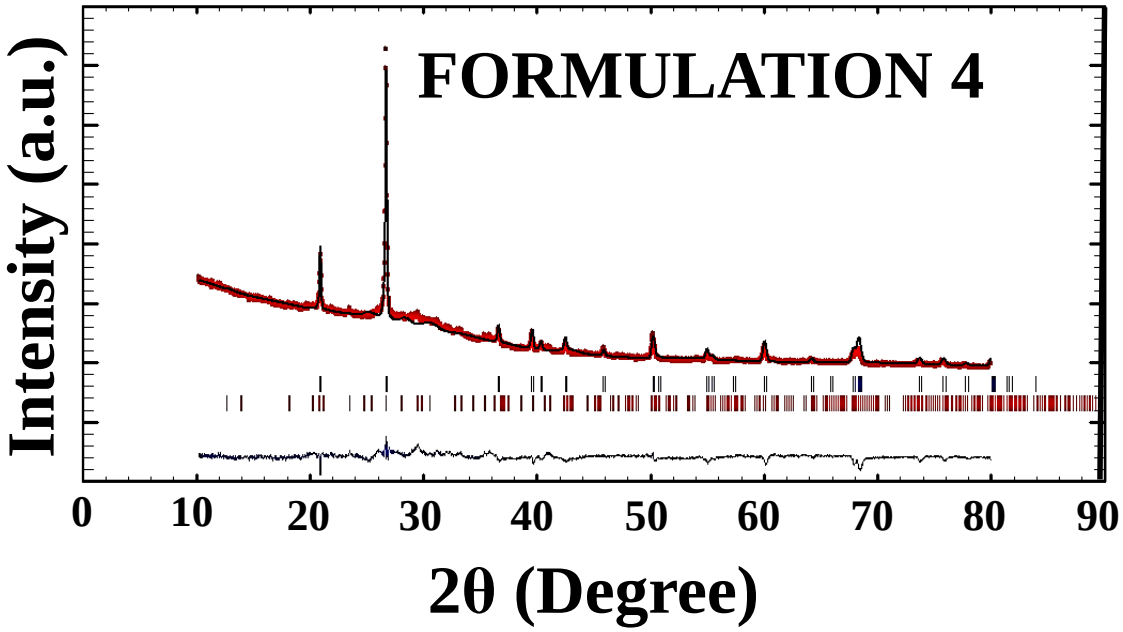

Figure 15 (continued). Rietveld refinement of the geopolymeric pastes.

3.3 Geopolymeric and ordinary mortars.

3.3.1 Compressive strength.

Figure 16 shows the compression tests results of ordinary and geopolymeric mortars after 7, 14 and 28 days of curing.

The results show that no geopolymeric mortars matched or exceeded the compressive strength of the ordinary mortars, excepting that of the formulation 6. However, formulations 8 and 9 were the geopolymeric mortars with the highest compressive strength.

The reason of those results is explained and discussed in the XRD analyses on section 3.3.2.

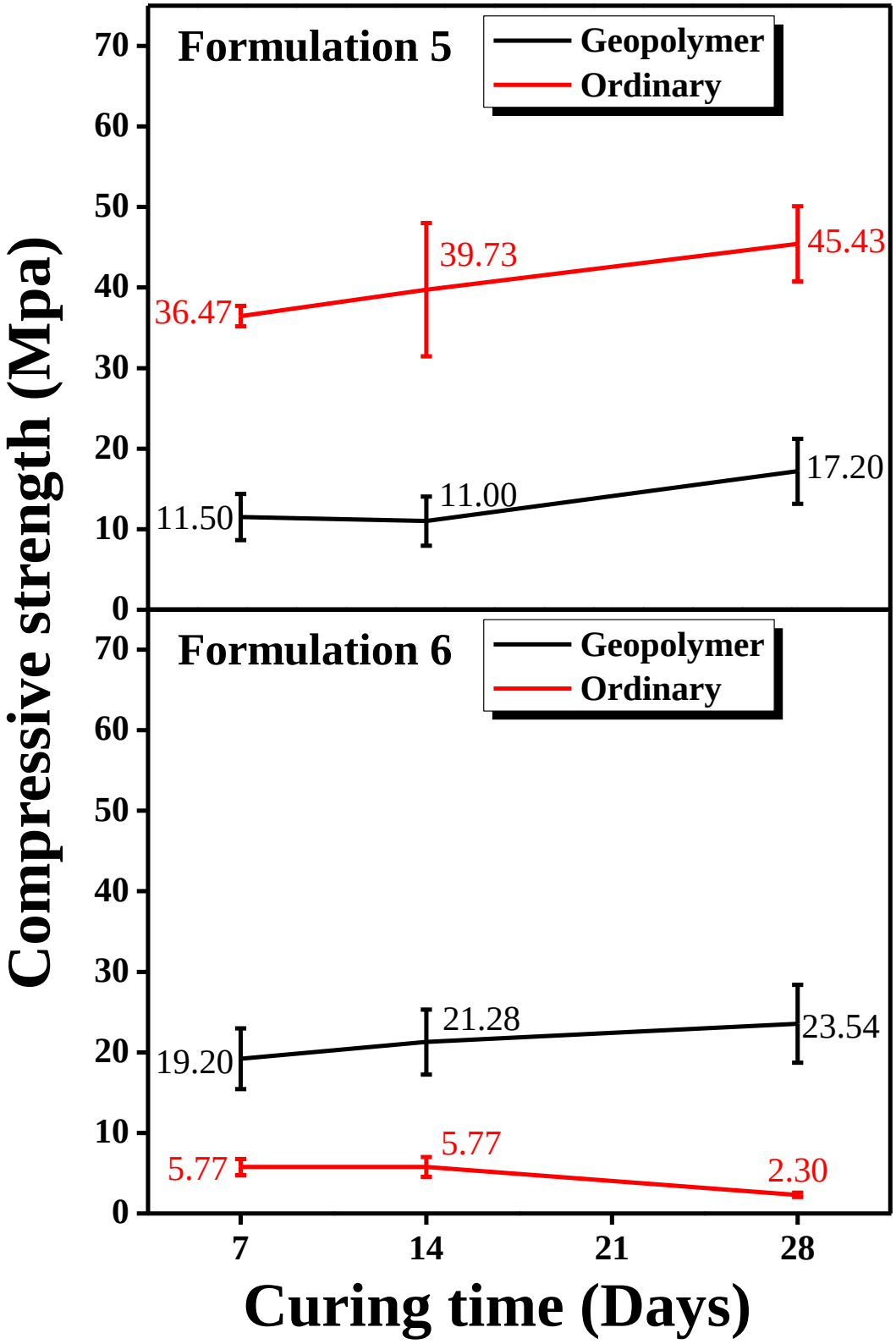

Figure 16. Compressive strength of the geopolymeric and ordinary mortars (continued on next page).

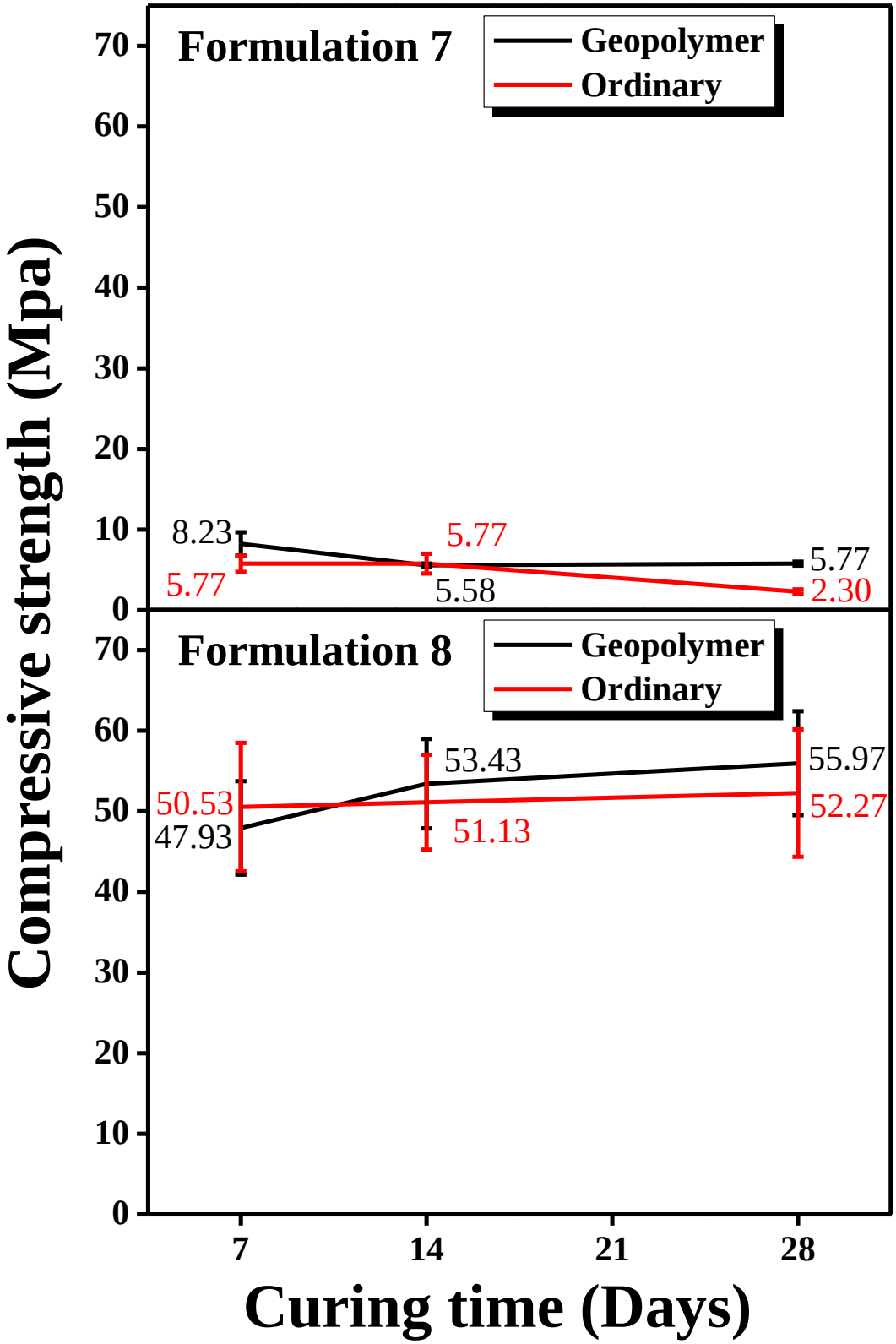

Figure 16 (continued). Compressive strength of the geopolymeric and ordinary mortars (continued on next page).

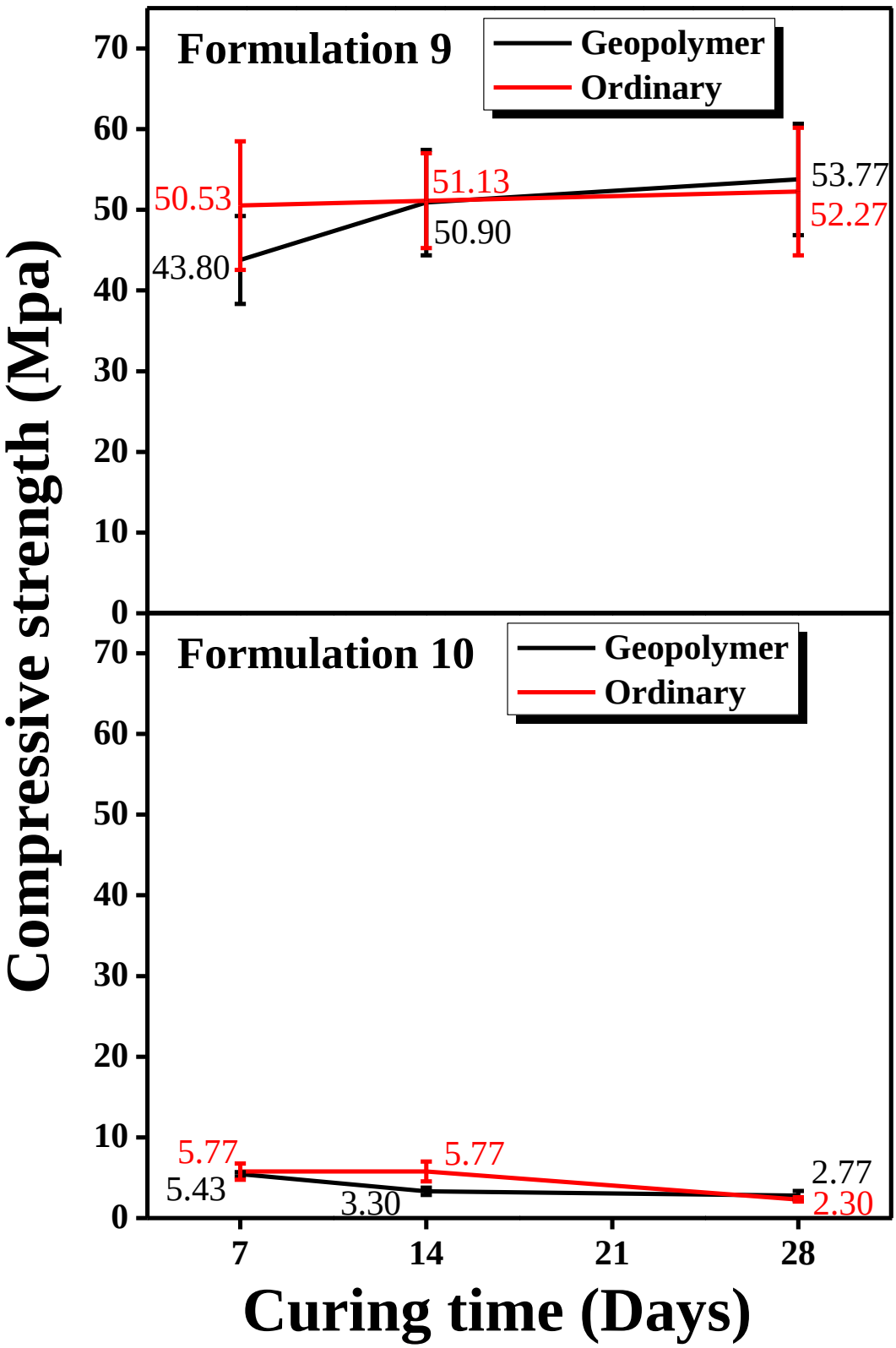

Figure 16 (continued). Compressive strength of the geopolymeric and ordinary mortars.

3.3.1.1 Effect of the particle size of clinker on the compressive strength.

Figure 17 shows the compressive strength of geopolymeric mortars by reducing the clinker particle size to 15 and 130 µm after 7, 14 and 28 days of curing.

The mortars of formulations 6, 7 and 10 could not be measured at 130 µm-particle size due to the lack of compaction of the materials. Their compressive strength at 15 µm is showed in Figure 16.

With those results, it is demonstrated the importance of having in these formulations a particle size distribution of clinker as small as possible. Large particle sizes will cause low compaction of the material and a reduced surface area for carrying out the geopolymerization reaction, resulting in a low compressive strength.

In previous works, it has been demonstrated that the particle size distribution of the raw materials has an important component on the compressive strength of geopolymers [40-42].

A decrease in particle size leads to an increase in the compressive strength [40].

The effect of particle size acts in two ways: during the mixing of the geopolymer, the activator solution demand rises as the particle size of the fly ash increases due to the need to fill larger voids among coarser fly ash particles to achieve a workable material [40].

On the other hand, when the particle size is small, the surface area will increase, resulting in a more reactive fly ash or, in this case, the clinker [40]. Much of the reaction occurs at the particle-liquid interface [40].

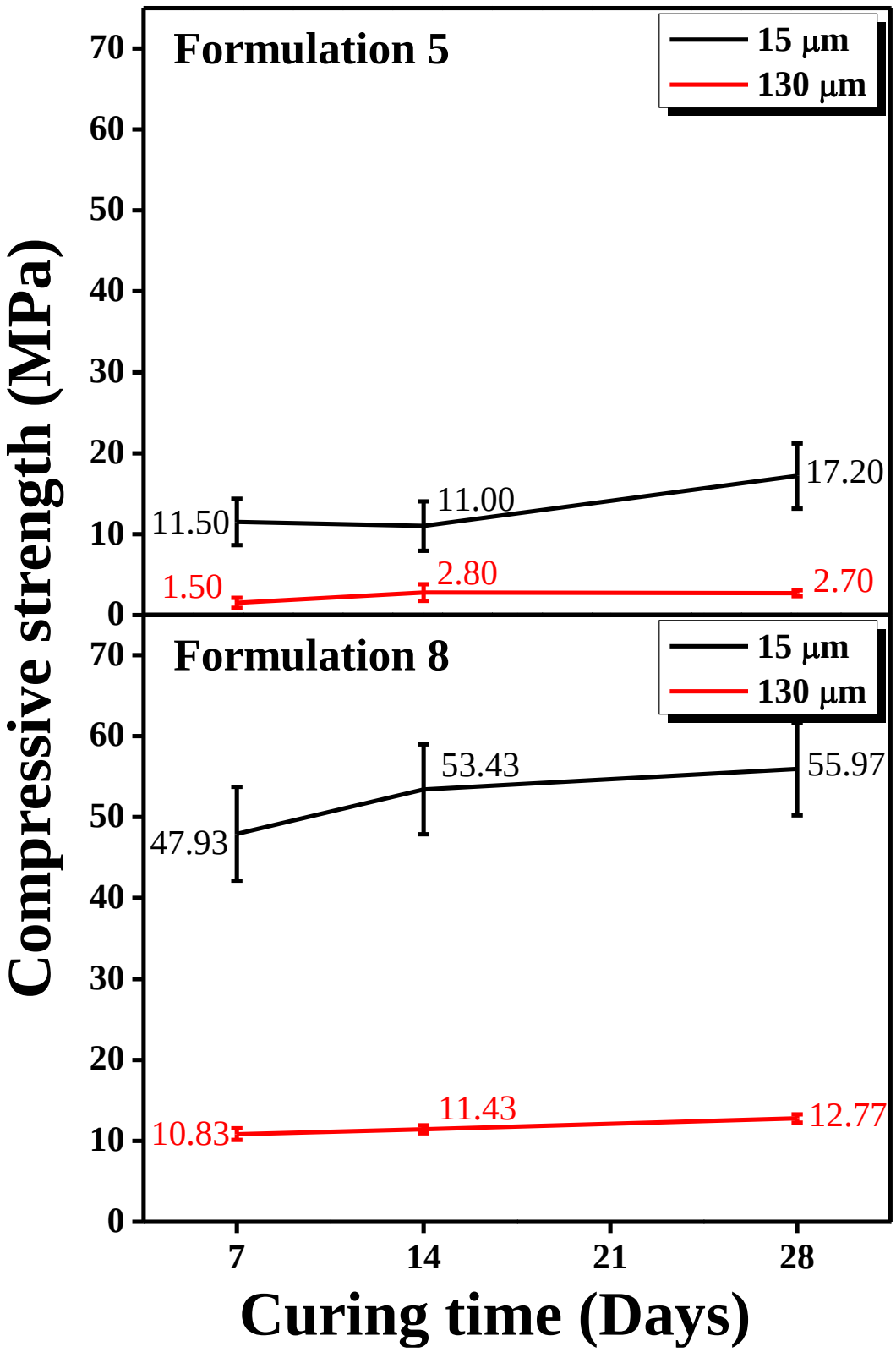

Figure 17. Compressive strength by reducing clinker particle size to 15 and 130 μm of the mortars (continued on next page).

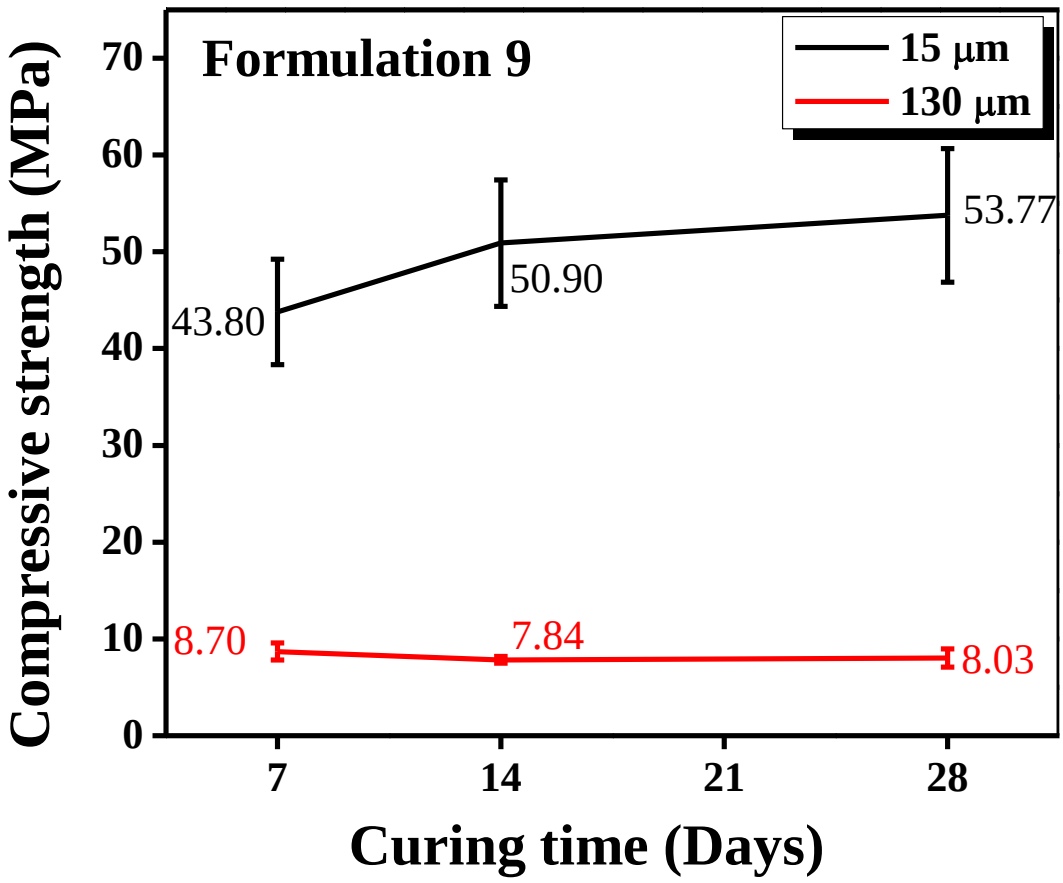

Figure 17 (continued). Compressive strength by reducing clinker particle size to 15 and 130 µm of the mortars.

3.3.1.2 Effect of dissolving the Pentasil® and/or sodium silicate in water on the compressive strength.

Figure 18 shows the compressive strength of the geopolymeric pastes after 7, 14 and 28 days of curing, having the Pentasil® and sodium silicate dissolved and undissolved in water.

Those results revealed the importance of dissolving the activators in water to increase the surface area and hence complete the geopolymerization reaction.

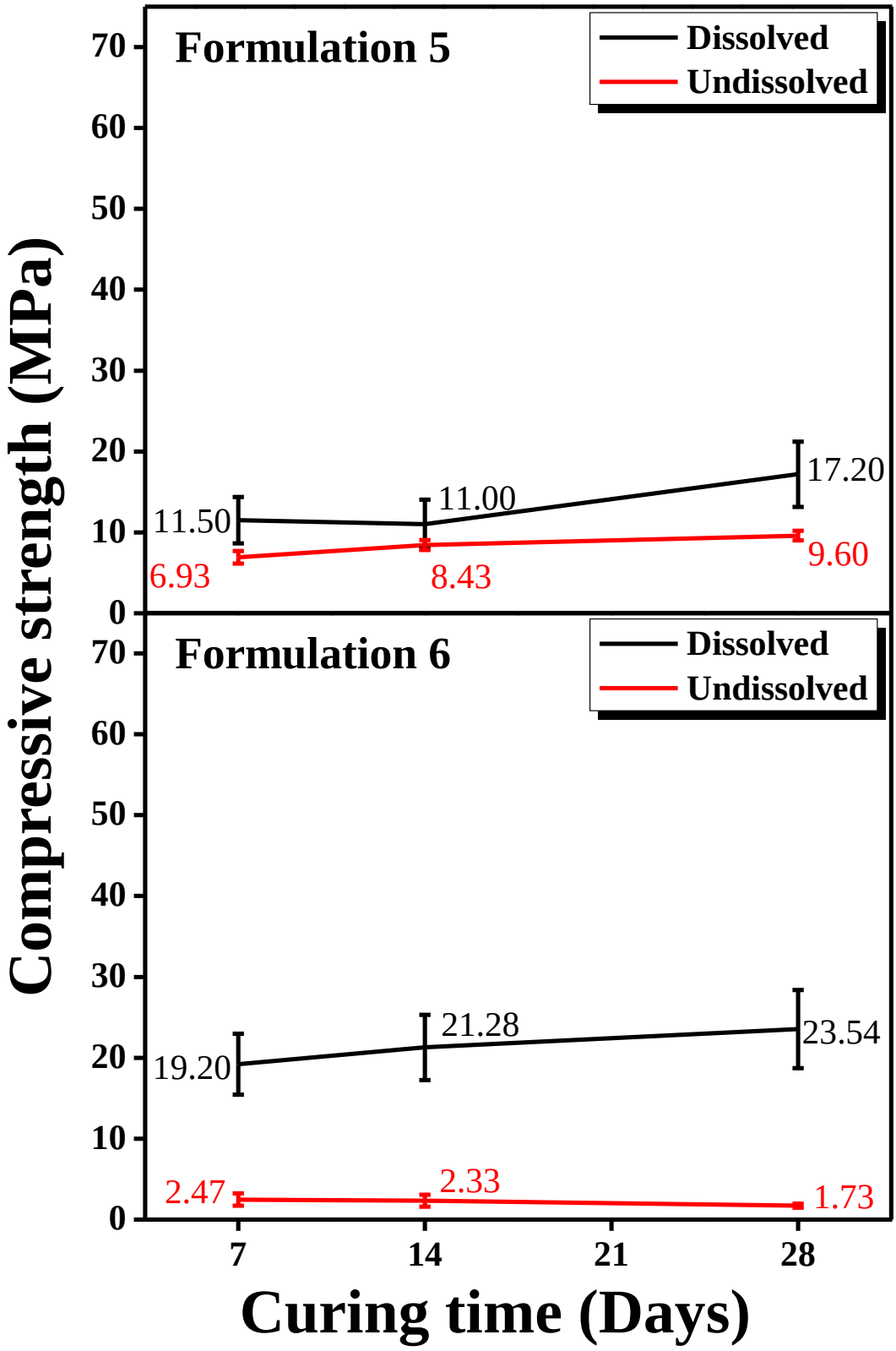

Figure 18. Compressive strength with Pentasil® and/or sodium silicate dissolved and undissolved in water of the mortars (continued on next page).

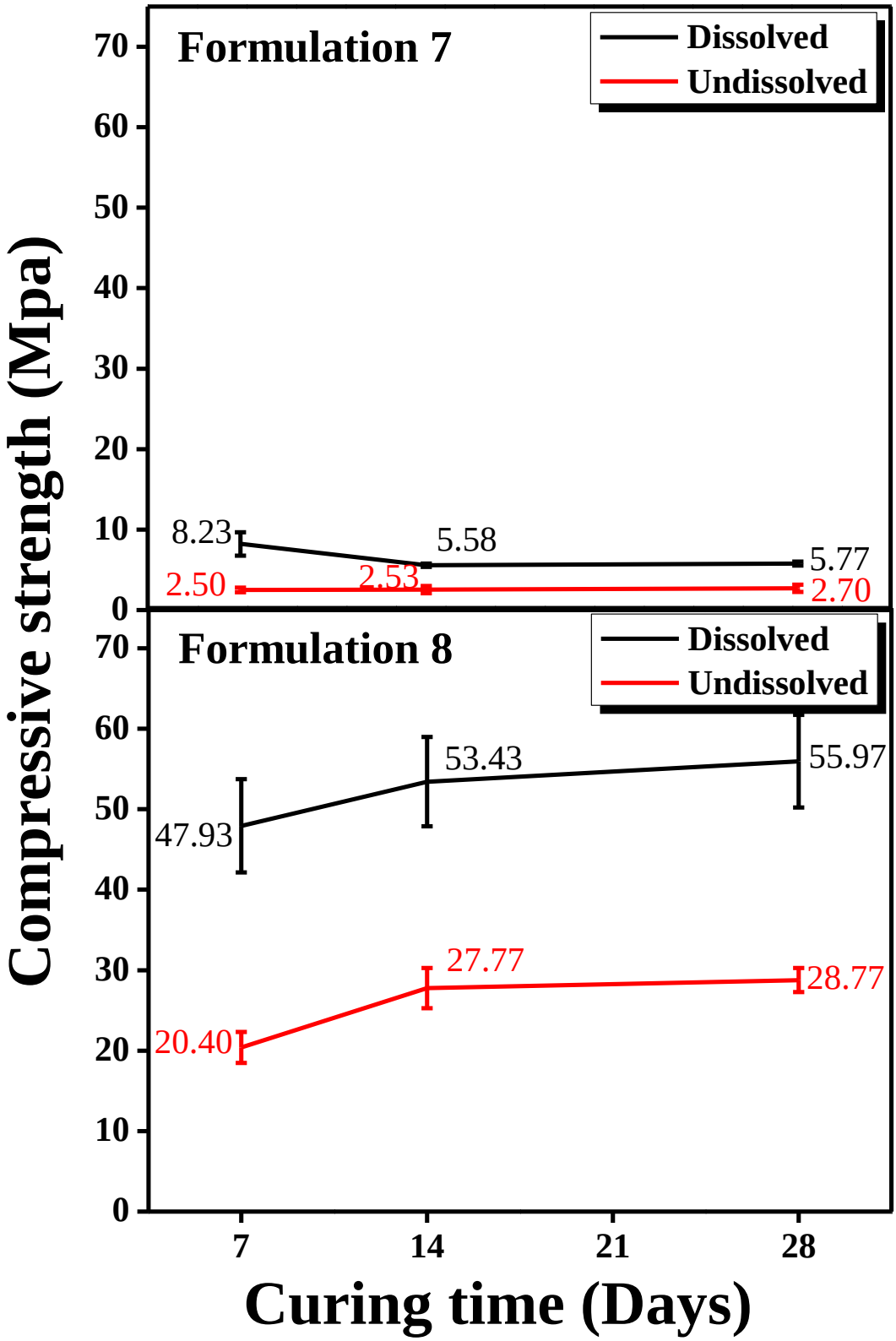

Figure 18 (continued). Compressive strength with Pentasil® and/or sodium silicate dissolved and undissolved in water of the mortars (continued on next page).

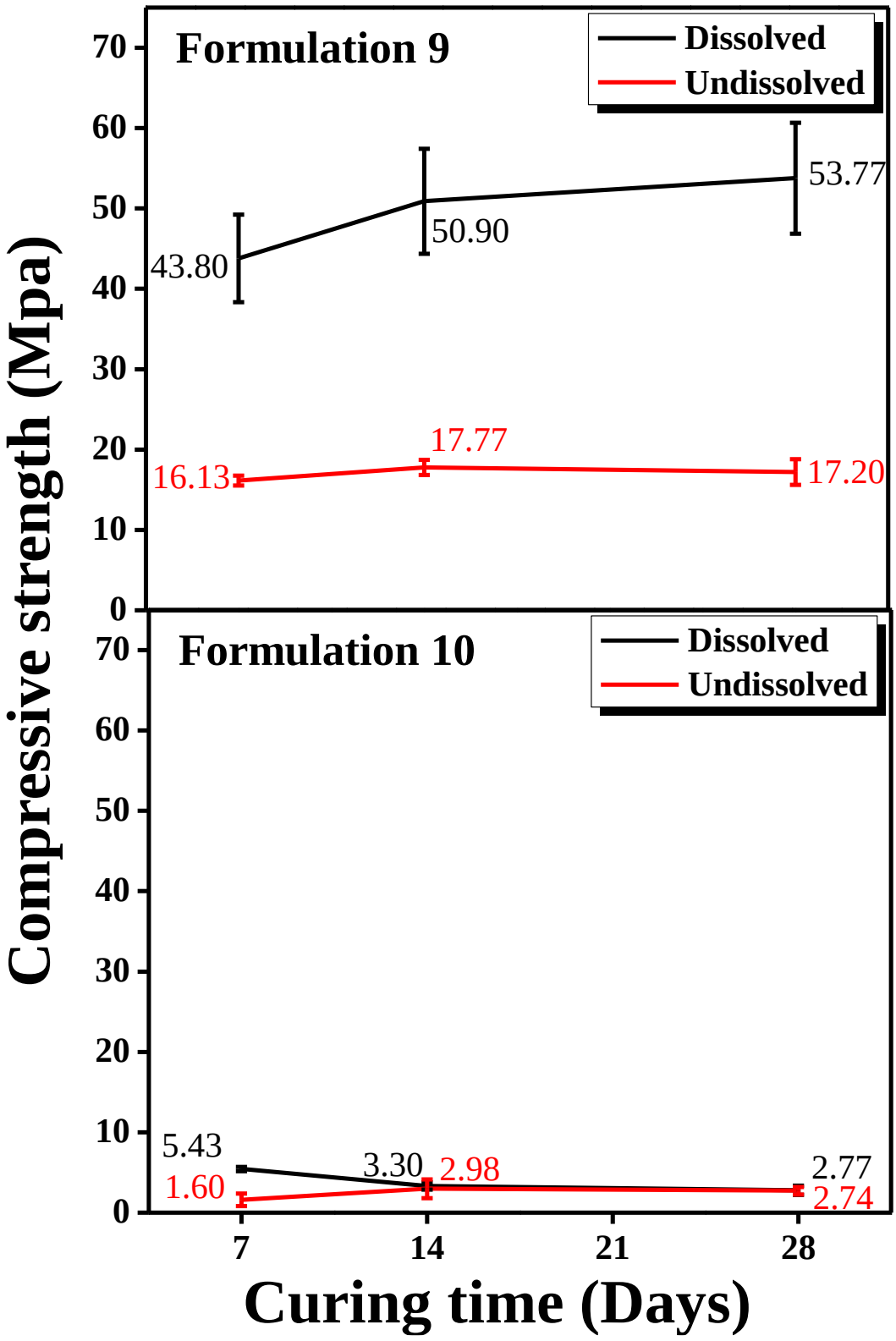

Figure 18 (continued). Compressive strength with Pentasil® and/or sodium silicate dissolved and undissolved in water of the mortars.

3.3.2 X-ray diffraction.

A qualitative XRD analysis was performed in order to know the phases present in each geopolymeric mortar. XRD patterns are illustrated in Figure 19. All the XRD patterns, except formulation 6, reveal the presence of alite and amorphous material in smaller amount than the pastes. This reduction of alite and content of amorphous material was due to the increase of quartz contained in the sand to successfully synthesize mortars. Table 12 shows the general information of these XRD patterns.

Formulation 5 and 6 demonstrated to have a similar performance than formulation 2 and 3. Formulation 5 did not have a compressive strength as high as the ordinary mortar, but, as was previously said, it can be used for other applications (e.g. sidewalks or rooms). Formulation 6 can be also used in those applications. Formulation 7 and 10 did not prove to have a favorable composition as was previously seen in formulation 4 but, in the case of the mortars, it was due to the excess of sand. These mortars were crumbled because of the lack of compaction, which resulted in a low compressive strength. However, XRD patterns of formulation 7 and 10 show to have small quantities of alite. Thus, it is possible to increase the compressive strength by decreasing the amount of sand. Finally, formulation 8 and 9 had the highest compressive strength of the mortars. It is attributed to the presence of alite as was previously seen in formulation 1. In fact, the XRD patterns of these formulations match with the pattern of formulation 1 (Figure 14).

Table 12. XRD pattern information of the geopolymeric mortars.

Formulation	Phases	Chemical formula	Crystalline system	MI color
5, 7-10	Alite Quartz	$3CaO{\cdot}SiO_2$ SiO_2	Monoclinic Trigonal	Red Black
6	Portlandite Quartz	$Ca(OH)_2$ SiO_2	Trigonal Trigonal	Green Black

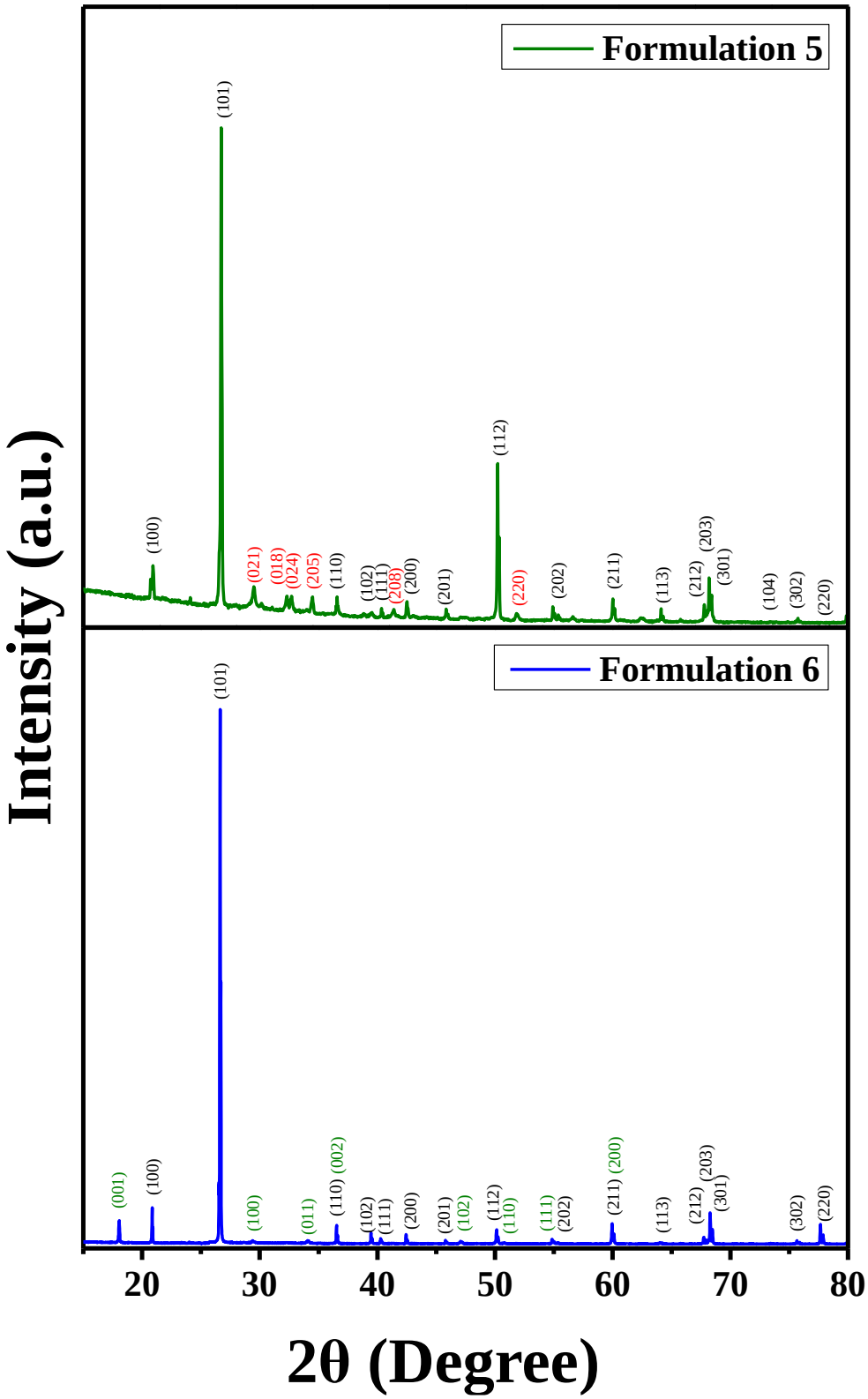

Figure 19. XRD patterns of the geopolymeric mortars (continued on next page).

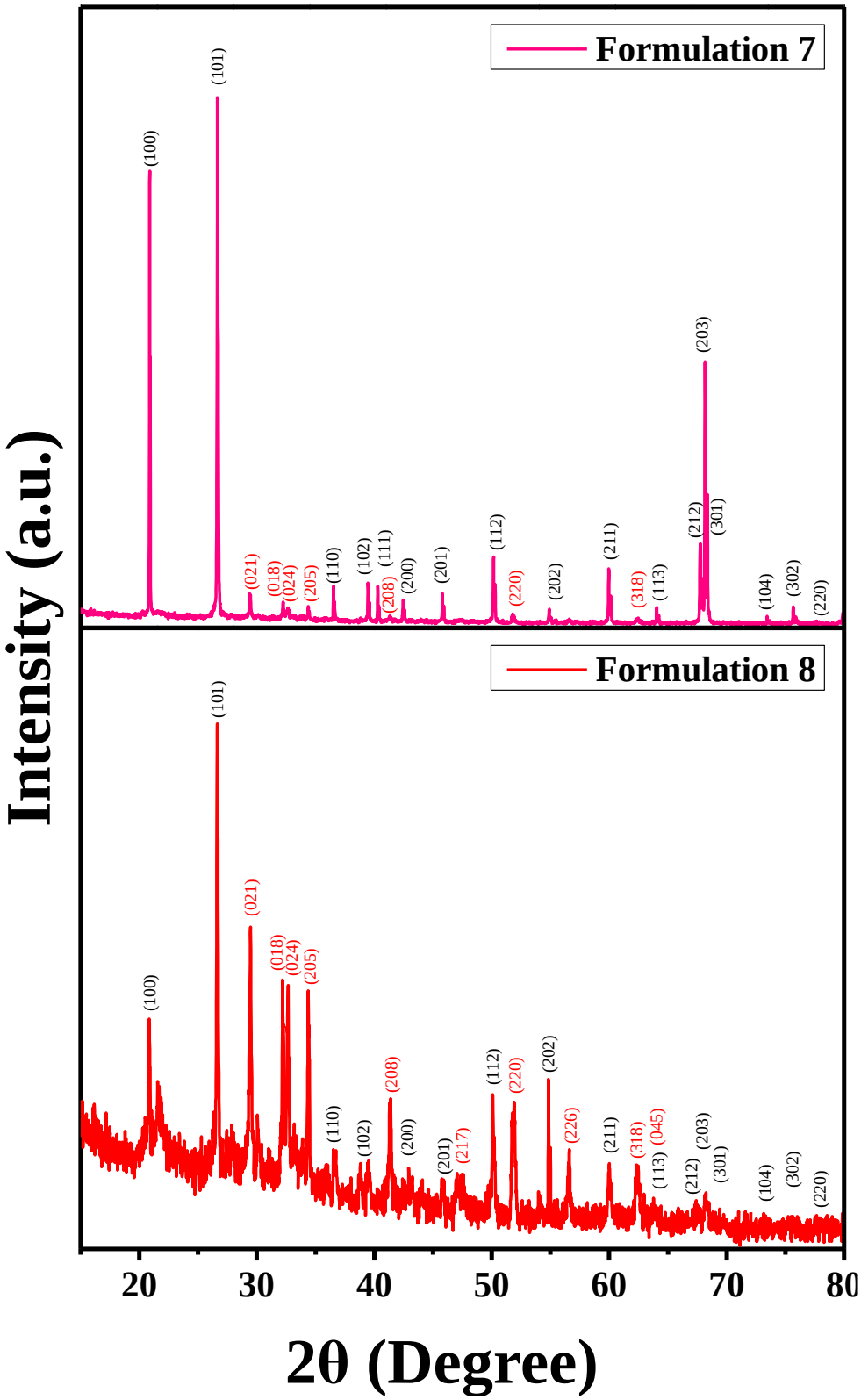

Figure 19 (continued). XRD patterns of the geopolymeric mortars (continued on next page).

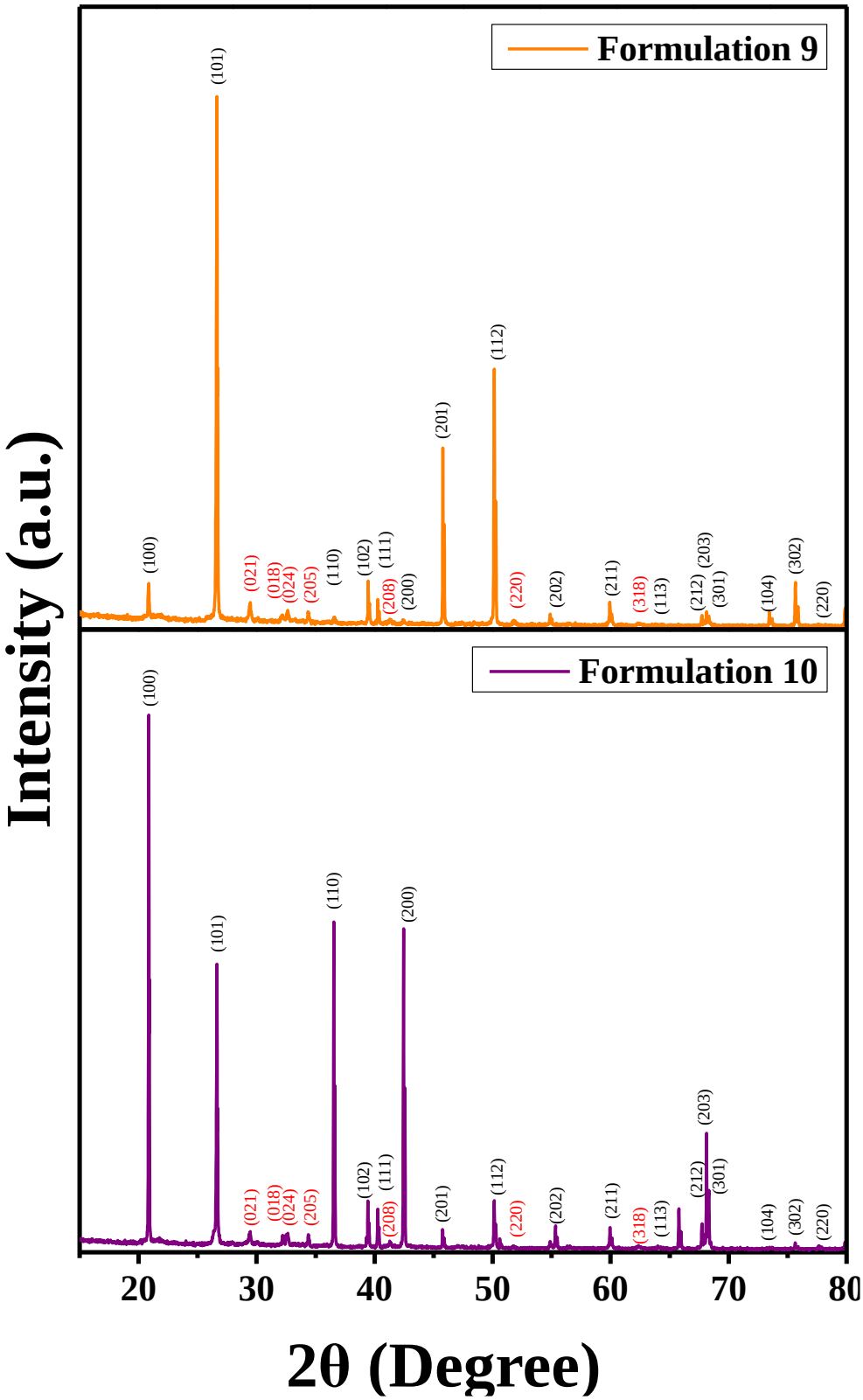

Figure 19 (continued). XRD patterns of the geopolymeric mortars.

CONCLUSIONS AND FUTURE WORK

Conclusions.

This research work was focused on the synthesis of geopolymeric materials, as well as on the comparison of their compressive strengths with ordinary materials.

It could be seen the importance of having small particle size in the raw materials in order to complete the geopolymerization reaction.

The compressive strength of the geopolymers increased by dissolving the Pentasil® and sodium silicate in water, which increased the surface area.

The Rietveld method was performed to analyze both the raw materials and geopolymeric pastes. The method allowed quantitatively estimating the phase composition in the investigated materials. The methodology developed by this method allowed understanding the relationship between the crystalline structure and the mechanical behavior under compressive loads of samples.

The geopolymeric paste with the highest compressive strength was the formulation 1, which contains 65 wt% of alite. Alite phase contributes to the development of early compressive strength of cement (generally in the first 28 days), working as a nucleating agent.

The Rietveld method is a labour-intensive task, especially when the number of phases increases. However, the established methodology in this work led to predict, from a qualitative XRD analysis, if the sample would have high or low compressive strength.

Future work.

1. To improve formulations in order to enhance the compressive strength of geopolymers.
2. To continue with the Rietveld analysis of mortars.
3. To evaluate the properties of the geopolymers by other techniques as setting time, drying shrinkage, expansion in autoclave, expansion in water, resistance with acids and alkalis.
4. To evaluate the mechanical properties of the geopolymers with no addition of clinker and carrying out a heat treatment for curing.
5. To synthesize the same formulations using a different calcium-rich component such as ground granulated blast furnace slag, calcium hydroxide or lime.

REFERENCES

1. Schneider, M., et al., *Sustainable cement production-present and future.* Cement and Concrete Research, 2011. **41**(7): p. 642-650.
2. Nowak, R., *Geopolymer concrete opens to reduce CO_2 emissions.* The New Scientist, 2008. **197**(2640): p. 28-29.
3. Kong, D.L. and J.G. Sanjayan, *Effect of elevated temperatures on geopolymer paste, mortar and concrete.* Cement and Concrete Research, 2010. **40**(2): p. 334-339.
4. Mendes, A., J. Sanjayan, and F. Collins, *Phase transformations and mechanical strength of OPC/Slag pastes submitted to high temperatures.* Materials and Structures, 2008. **41**(2): p. 345-350.
5. Fuentes, L., *Introducción al método de Rietveld.* Centro de Investigación de Materiales Avanzados, SC Editorial IFUNAM, México DF, 2002.
6. Ortuño, Á.V., *Introducción a la química industrial*. 1998, Barcelona, España: Reverté.
7. Eckel, E.C., *Portland cement materials and industry in the United States*. 1913: US Government Printing Office.
8. Newman, J. and B.S. Choo, *Advanced Concrete Technology*. Vol. 4. 2003: Butterworth-Heinemann.
9. Provis, J. and J. Van Deventer, *Geopolymers: structure, processing, properties and industrial applications. 2009*. Woodhead Publishing Limited.
10. McLellan, B.C., et al., *Costs and carbon emissions for geopolymer pastes in comparison to ordinary portland cement.* Journal of Cleaner Production, 2011. **19**(9): p. 1080-1090.

11. Singh, B., et al., *Geopolymer concrete: a review of some recent developments.* Construction and Building Materials, 2015. **85**: p. 78-90.

12. Troitzsch, J. and J. Troitzsch, *Plastics flammability handbook*. 2004: Carl Hanser Verlag GmbH & Co. KG München.

13. Davidovits, J., *Geopolymer Chemistry and Applications. Saint-Quentin, FR: Geopolymer Institute*. 2008, ISBN 978-2-9514820-1-2.

14. Rowles, M. and B. O'connor, *Chemical optimisation of the compressive strength of aluminosilicate geopolymers synthesised by sodium silicate activation of metakaolinite.* Journal of Materials Chemistry, 2003. **13**(5): p. 1161-1165.

15. Guiping, L., *Material and Manufacturing Technology II: Selected, Peer Reviewed Papers from the 2011 2nd International Conference on Material and Manufacturing Technology (ICMMT 2011), July 8-11, 2011, Xiamen, China*. 2012: Trans Tech Publications.

16. Tejeda, A., *Synthesis and characterization of sodium silicate obtained by different chemical routes. Master thesis, CIMAV.* 2015: México.

17. Dimas, D., I. Giannopoulou, and D. Panias, *Polymerization in sodium silicate solutions: a fundamental process in geopolymerization technology.* Journal of Materials Science, 2009. **44**(14): p. 3719-3730.

18. Rahier, H., B. Van Mele, and J. Wastiels, *Low-temperature synthesized aluminosilicate glasses.* Journal of Materials Science, 1996. **31**(1): p. 80-85.

19. Jamieson, E., et al., *Optimising ambient setting Bayer derived fly ash geopolymers.* Materials, 2016. **9**(5): p. 392-403.

20. Rovnaník, P., *Effect of curing temperature on the development of hard structure of metakaolin-based geopolymer*. Construction and Building Materials, 2010. **24**(7): p. 1176-1183.

21. Van Deventer, J., et al., *Reaction mechanisms in the geopolymeric conversion of inorganic waste to useful products.* Journal of Hazardous Materials, 2007. **139**(3): p. 506-513.

22. Duxson, P., et al., *Geopolymer technology: the current state of the art.* Journal of Materials Science, 2007. **42**(9): p. 2917-2933.

23. Settlements, U.N.C.f.H., *Small-scale Production of Portland Cement*. 1993: United Nations Centre for Human Settlements (Habitat).

24. Will, G., *Powder Diffraction : The Rietveld Method and the Two Stage Method to Determine and Refine Crystal Structures from Powder Diffraction Data*. Vol. 1. 2006, Berlin, Heidelberg: Springer.

25. N/A, *ICAM 2008 - Ninth International Congress for Applied Mineralogy Conference Proceedings*. The Australasian Institute of Mining and Metallurgy (The AusIMM).

26. Harper, M. and T. Lee, *5.3.1 Quantitative Characterization of Bulk Samples Using the Rietveld Method*, in *Silica and Associated Respirable Mineral Particles - (STP 1565)*. ASTM International.

27. Lutterotti, L., et al. *Quantitative analysis of silicate glass in ceramic materials by the Rietveld method*. in *Materials Science Forum*. 1998. Aedermannsdorf, Switzerland: Trans Tech Publications, 1984-.

28. Scientifiques, E. *ES-France*. 2012; Available from: http://www.es-france.com/pdf/1180_us_doctech.pdf.

29. Barbosa, V.F., K.J. MacKenzie, and C. Thaumaturgo, *Synthesis and characterisation of materials based on inorganic polymers of alumina and silica: sodium polysialate polymers.* International Journal of Inorganic Materials, 2000. **2**(4): p. 309-317.

30. Callister, W.D. and D.G. Rethwisch, *Materials science and engineering*. Vol. 5. 2011: John Wiley & Sons NY.

31. Balandrán, M., *Sintesis de geopolímeros mediante diferentes precursores. Tesis de Maestría.* 2011, Universidad Autónoma de Nuevo León: México.

32. Silva, P.D., K. Sagoe-Crenstil, and V. Sirivivatnanon, *Kinetics of geopolymerization: Role of Al2O3 and SiO2.* Cement and Concrete Research, 2007. **37**(4): p. 512-518.

33. Wang, G.Y., L.C. Lu, and S.D. Wang. *Effects of Shell and Calcium Carbonate on Properties of Portland Cement*. in *Advanced Materials Research*. 2012. Trans Tech Publ.

34. Celik, I.B., *The effects of particle size distribution and surface area upon cement strength development.* Powder Technology, 2009. **188**(3): p. 272-276.

35. Provis, J., et al., *Analysing and manipulating the nanostructure of geopolymers*, in *Nanotechnology in Construction 3*. 2009, Springer. p. 113-118.

36. Alsop, P.A., et al., *Cement Plant Operations Handbook: For Dry Process Plants*. 2007: Tradeship.

37. Parrot, L. and D. Killoh. *Prediction of cement hydration*. in *Proceedings of the British Ceramic Society.* 1984.

38. Benites Espinoza, C.M., *Concreto (hormigón) con cemento Pórtland Puzolánico tipo IP Atlas de resistencias tempranas con la tecnología SIKA Viscocrete 20HE.* 2011.

39. Guo, X., H. Shi, and W.A. Dick, *Compressive strength and microstructural characteristics of class C fly ash geopolymer.* Cement and Concrete Composites, 2010. **32**(2): p. 142-147.

40. Gunasekara, C., et al., *Zeta potential, gel formation and compressive strength of low calcium fly ash geopolymers.* Construction and Building Materials, 2015. **95**: p. 592-599.

41. van Jaarsveld, J.G.S., J.S.J. van Deventer, and G.C. Lukey, *The characterisation of source materials in fly ash-based geopolymers.* Materials Letters, 2003. **57**(7): p. 1272-1280.

42. Fernández-Jiménez, A. and A. Palomo, *Characterisation of fly ashes. Potential reactivity as alkaline cements.* Fuel, 2003. **82**(18): p. 2259-2265.